# Tubular Shaped (Continuum) Soft Robotic Arm with Variable Stiffness: Design, Fabrication, and Testing

An Undergraduate Honors Thesis

Presented in Partial Fulfillment of the Requirements for Graduation with Distinction in the

Department of Mechanical Engineering at The Ohio State University

By

Qihang Zeng
Undergraduate Honors Program in Mechanical Engineering

The Ohio State University

2019

Undergraduate Honors Thesis Committee

Dr. Haijun Su, Advisor

Dr. Sandra Metzler, Committee Member

**Abstract**

Soft robots are designed to be highly flexible and adaptable to their surroundings. Often times conventional rigid robots are at a disadvantage due to lack of versatility in complex environments and safety concerns on human-robot interactions. Soft robots can be compliantly designed to overcome those limitations at the expense of lower precision and reduced load capacity. To improve the precision and weight carrying capability, this research built a compliant robotic arm of tunable stiffness by using layer jamming technique. Most of continuum and compliant robotic arm designs have a center backbone, which connects the subsections and provides the majority of the stiffness. However, the center backbone takes large internal space of the robotic arm which could be used for wiring and sensor/gadget placement. This research project provided a tubular shaped solution by redesigning the backbone and placing the compliant backbone at the perimeter of each tubular subsection, thus leaving large space available inside the robotic arm. With the novel body design and the incorporation of layer jamming, the arm is able to pass through complex environment to reach target locations with its compliant body, that contains 3 subsections with 90 degrees maximum bending angle on each. Stiffness can be tuned up to 87 times higher in high stiffness mode (12.5psi vacuum pressure) than its natural state (0psi). This robotic arm is able to eliminate or reduce impact injury in its low stiffness mode and perform accurately while carrying large load in its high stiffness mode. The features of this robotic arm give benefit in minimal invasive surgery and rescue robotics applications.

**Acknowledgements**

This project would not be possible without the support I received from others. I would like to thank my advisor, Dr. Haijun Su for giving me the opportunity to work on this fascinating project. He guided me during the 2 years of me work in Design Innovation and Simulation, giving suggestions to technical issues I encountered, and provided me with all needed equipment.

I would like to thank graduate student Xianpai Zeng for his guidance in layer jamming process and fabrication techniques, as well as resources for me to familiarize the facilities at DISL.

I would like to thank graduate student Yuan Gao for giving advice in setting up stiffness test for tubular shaped robotic arm.

I would also like to thank visiting scholar Zeyi Yang, for helping me design vacuum bag layout for layer jamming.

Finally, I would like to thank my parents, who continuously supported me morally and financially. Their help was crucial to the success of this project.

## Table of Contents

## Table of Figures

# Chapter 1: Introduction

## 1.1 Soft Robotics

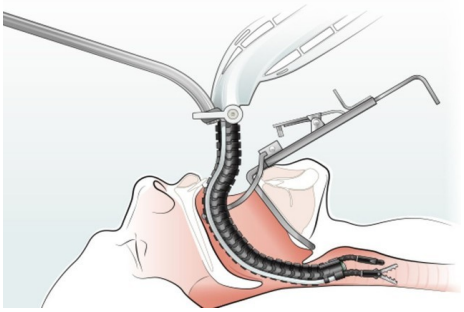

*Figure 1: Continuum Soft Robot perform Surgery [1]*

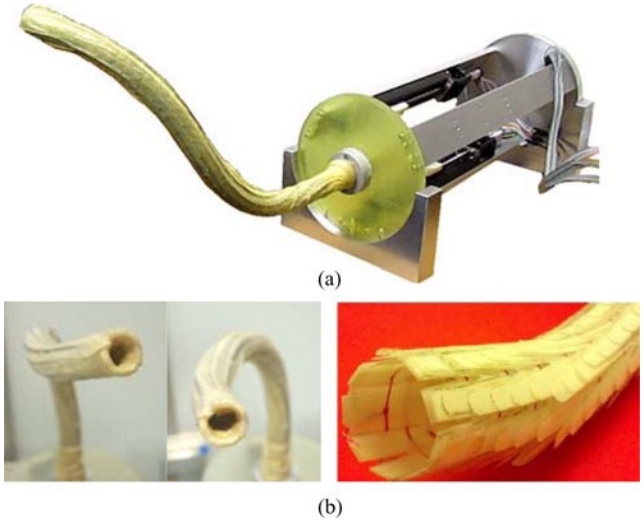


*Figure 2: A Current State of Art of Continuum Robotic Arm [7]*

Conventional robots are constructed with discrete rigid linkages connected by joints with finite numbers of DOF (Degree of Freedom). Many are designed to focus on precision and/or power at the end-effector, over interactions of the robotic body and its surroundings. As the need of flexibility and adaptability in numerous applications has developed in recent decades, meanwhile the number of safety accidents occurs with robotic arms, physical constraints of rigid body robotics presented limitations in applications such as minimally invasive surgery (fig.1) [1] and complex mechanical system maintenance [2]. The concept of soft robotics emerged when Anderson and

Horn introduced the Tensor Arm [3]. Soft robots have two distinct design approaches: (1) link-compliancy robotic manipulators [4] and (2) joint-compliancy robots with rigid-link (fig.2) [5] [7]. The former approach design and fabricate robotic components fully utilizing compliant materials such as directional adhesive grippers [6] and multigait soft robots [8]. The second approach defines a design of robotic arm with compliancy and capability to carry end-effectors. The soft materials allow the robot to conquer the natural drawback of rigid body robots and readily adapt to their surroundings. In addition, they reduce the damages to human body when accidental interaction occurs with machine, therefore enhance safety. The later approach is the focus of this thesis.

## 1.2 Variable Stiffness Technology

### 1.2.1 Variable Stiffness Advantage

While the soft robots perform extensively in complex environments, they have limited ability handling heavy payloads and high accuracy tasks. Due to soft robots' inherent propensity for deformation under load, soft robots are difficult to control accurately. An effective way to eliminate deformation effects requires integrating variable stiffness to the design, therefore combining the advantage of both soft and rigid robots. For instance, in minimal invasive surgeries, a robotic arm can be set to low stiffness mode, compliantly bypassing the organs and reach target position. When performing tasks, it can be set to high stiffness mode. With a more rigid body the robotic arm is capable of performing enhanced precision tasks and carrying elevated payload. In the recent years, co-robots are widely used in manufacturing field. They assist human workers to handle tasks that requires high power. This could be dangerous in human-robot corporation due to the complementary high strength of co-robots. Research shows that robotic arm with lower stiffness can reduce injure to human body [9][10]. However

due to the poor load carrying capability of soft robots, they are not exploited in manufacturing plants. This could be changed with the addition of variable stiffness. A co-robot can be tuned stiff while performing tasks where strength is needed, and when a collision is sensed the arm softens to reduce the damage to human workers, therefore provides them a safer working environment.

### 1.2.2 Antagonistic Arrangement Design

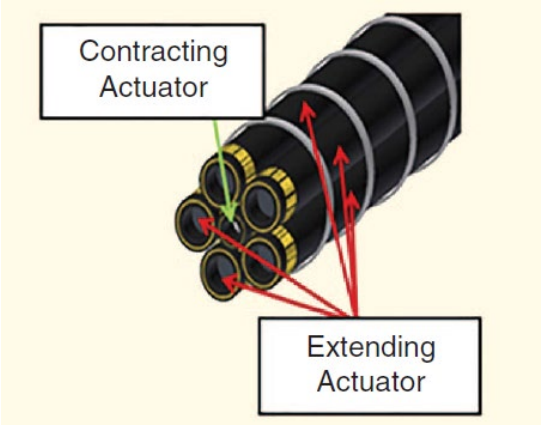


*Figure 3: Antagonistic Structured Variable-Stiffness Device [12]*

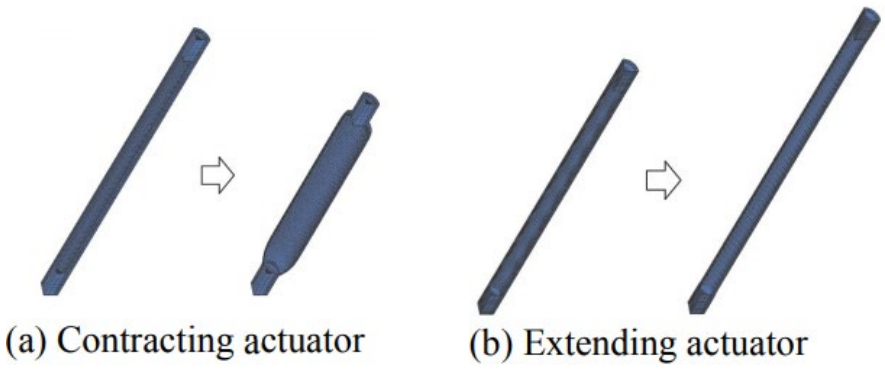


*Figure 4: Mechanism of (a) Contrasting Actuator (b) Extending Actuator [12]*

There are a few ways to adjust stiffness of a compliant structure. The first is to utilize antagonistic arrangement design [12]. It places active elements in contrast of each other or applies which to a passive structure such as a backbone. By stiffening the active elements, the overall stiffness of the system increases. As shown in figure 4, the expanding actuators are placed on the perimeter of the continuum robotic manipulator, with the contracting actuator in the center. By adding pressure, the extending actuator will elongate, and the contrasting actuator shortens (fig.5), thus the system can not only form a bend in the opposite direction of the actuated expending actuator, but also enhance the stiffness by increasing the pressure in all actuators. This is resulted by the contracting forces holding the shape of the robot. Although this method allows independent adjustment of stiffness and the equilibrium position of the system, it is difficult to accurately control the curvature of robotic arm in our application. In addition, the structure of this design restricts the inner space of the robotic arm, which runs counter to the goal of this thesis.

### 1.2.4 Jamming Based System

(a)Granular Jamming and Layer Jamming

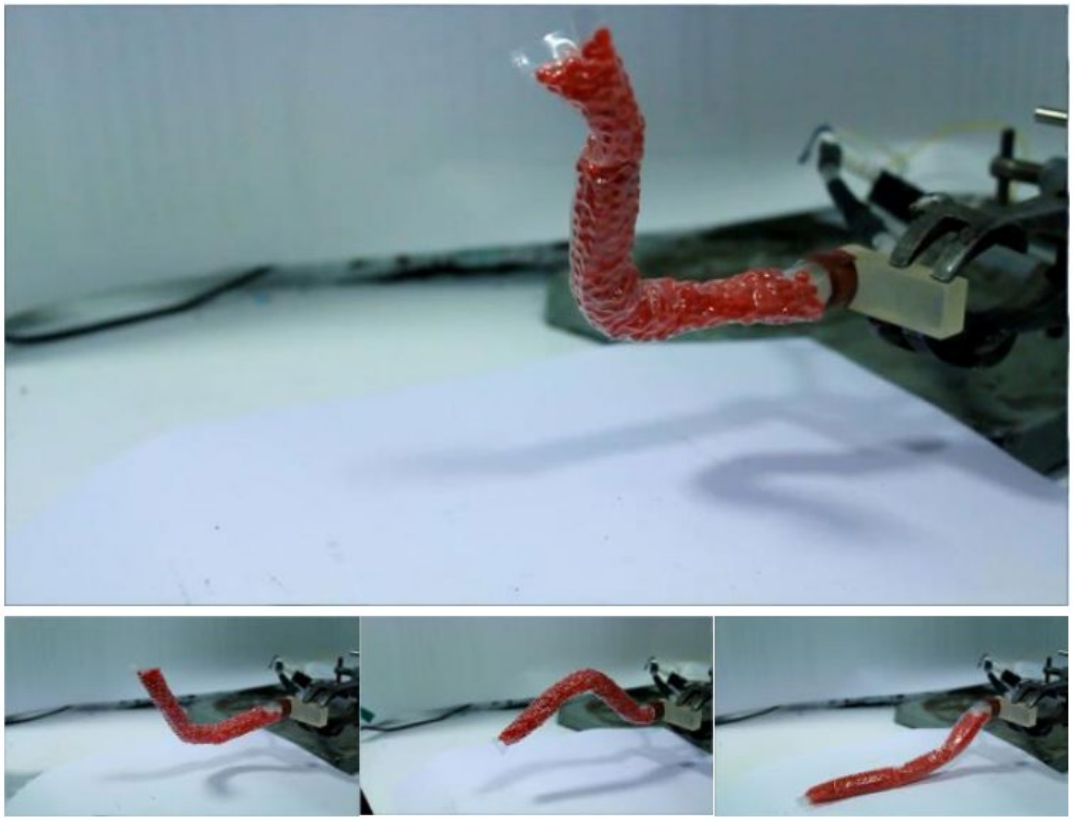

*Figure 5: Granular jamming Featured Variable-Stiffness Device [14]*

Another way of stiffening is by using jamming based system [13], with two approaches: granular jamming [14] (fig. 6) and layer jamming [15] [16] (fig. 7). Both are activated referring to the same principle: apply vacuum pressure to the jamming matter, which are attached to the compliant structure, thus developing a greater shear stress among the particles or layers. In this way the system stiffness is increased by constraining the relative motion among the backbone of the robotic arm. As shown in figure 8, the constraining force F is a friction force caused by the normal pressure P, which is resulted by the vacuum pressure. This determines the

increasing relationship between stiffness level and the vacuum pressure applied to the bag and endows the jamming-based system a high accuracy for tuning stiffness. Comparing to layer jamming system, granular jamming requires plenty of granular matter to realize significant stiffness fluctuation, while this thesis is focusing on building prototype in a small scale. Therefore, layer jamming becomes the ideal method of choice in this research project. Compared to granular jamming method, the overlapping layers of layer jamming has a much larger contacting surface for stiffening the target object and generate significant friction when applying negative air pressure. It provides comparatively outstanding stiffness ratio with a simple architecture.

(b)Layer Jamming for Tubular Shaped Backbone

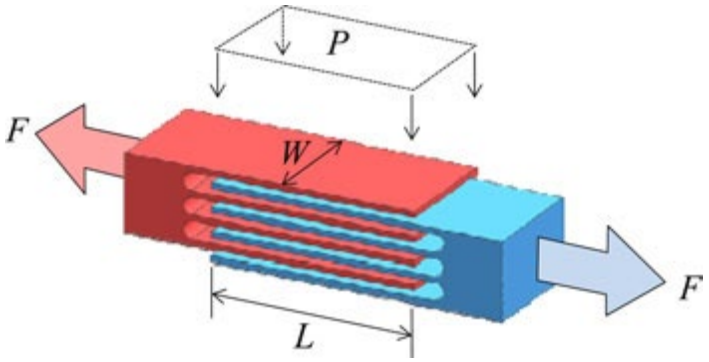


*Figure 6: Layer Jamming Variable Stiffness Mechanism [16]*

Previous studies have done in DISL to accomplished variable stiffness on cantilever beam and parallel guided beam shaped robotic arms. The rectangular one-piece layers work well on those planar motion robotic arms. They can achieve up to 70 times of stiffness change, nonetheless this outstanding design have a constraint in this thesis. This layer design only allows planar

bending motion and prevents any movement in other directions. Study in continuum robotic arm uses layer strips to wrap the perimeter of robotic link (fig.8). This layer shape solves the issue in the previous prototype. Meanwhile the interlocked layout requires large outer surface on the backbone links for installation. This thesis proposes a novel approach of layer layout by applying layer strips onto each robot link in the same direction.

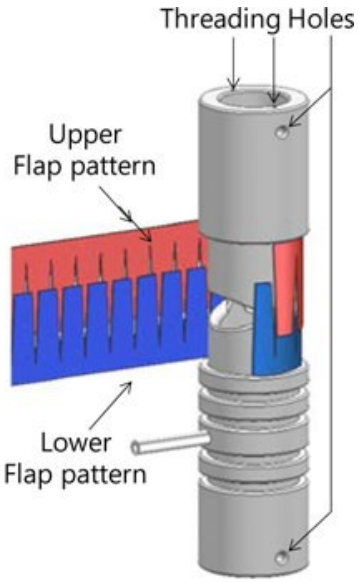


*Figure 7: Continuum Robotic Link with Strip Shaped Layers [16]*

## 1.3 Tubular Shaped Backbone

### 1.3.1 Tubular shaped Backbone Methodologies

Tubular shaped backbone design gives a large hollow space within the body of robotic arm. To achieve this, the compliant joints needs to place at the perimeter on the backbone. The resource of tubular shaped soft robotic arm is limited. The traditional way is to employ triangle notches to the continuum manipulator, where every section of the notch can be compressed or stretched to one direction and result in bending motion [17]. Although the simple structure was widely used in

tubular shaped continuum robot applications, the backbone design in this thesis requires capability of equipping layers and actuation materials, which the triangular notch backbone is lack of. In contrast, twin-pivoted backbone design (fig.9) [18] places compliant joints on the perimeter of each disk with 90 degrees alternation between two adjacent gaps. When a continuum robot contains an even number of gaps, it can have the equal amount of maximum bending angle in two perpendicular planes, and able to form bending in any direction by combining the motion in the two perpendicular directions. This design also provides sufficient space for actuation materials and layers while maintaining the equal inner space for other gadgets as the triangular notch design does.

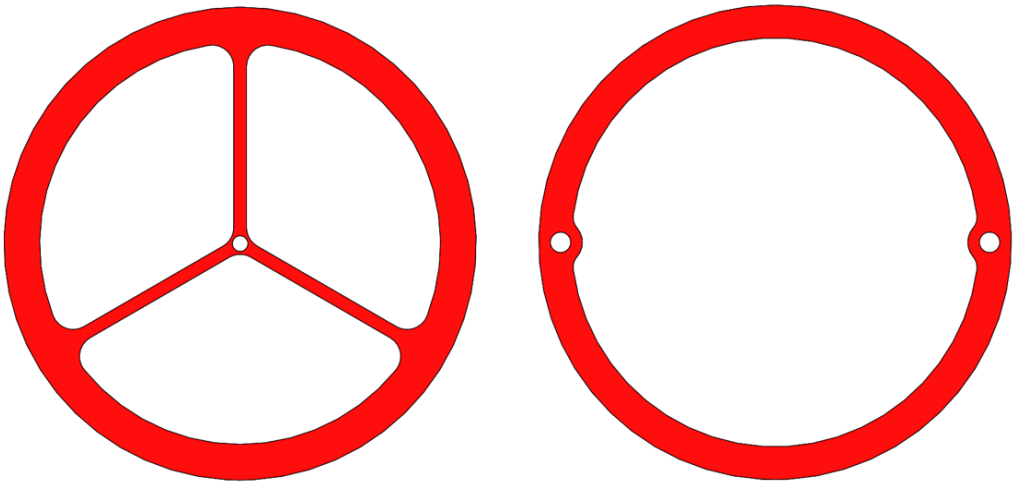

*Figure 8: Inner space Comparison between central backbone design (left) and twin pivoted design (right)*

### 1.3.2 Twin Pivoted Robotic Backbone Advantage

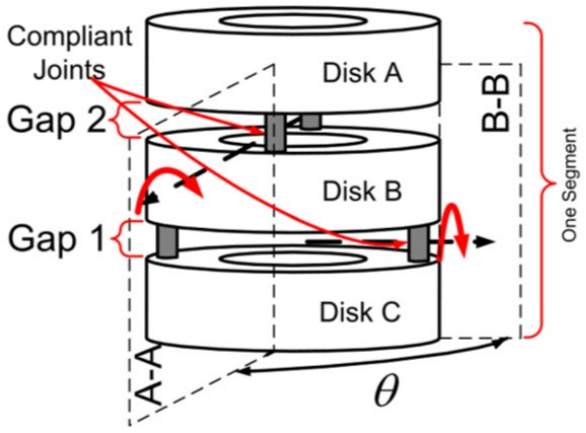


*Figure 9: Twin Pivoted Backbone Design [18]*

Central backbone designs [11] provide superior flexibility with a simple structure and have been adopted in the majority of research in continuous soft robotics. However, this design prevents pass-through of wires, sensors, and installation of end effectors. On the other hand, a tubular structural design circumvents the above issues, by providing a large cavity (fig.3). The increased inner space allows equipping integrated sensors, wires, and layer jamming vacuum bags inside the arm. Each segment has two joints for a planar bending motion, which also constrains the twist motion of the arm, thus reduces complexity in modeling and control.

## 1.4 Actuation Methodologies

### 1.4.1 pneumatic actuator

Pneumatic actuation controls the shape of a sealed structure by applying different air pressure. Applications such as pneumatic grippers [19] and air muscles (fig.10) [20] are commonly used in soft robotic field. Previous research has used air muscle to manipulate cantilever beam robotic arms by applying compressed air to air muscles to change the gap length on one side of the beam to result in bending motion. However, the slender shape of air muscles determines

the ineligibility in tubular shaped backbone applications. Due to the nature of pneumatic actuators, it is challenging to fabricate them to the scale that fits the prototype in this thesis. In addition, control of pneumatic actuators requires several valves to achieve bending in multiple directions. This adds complexity to the system.

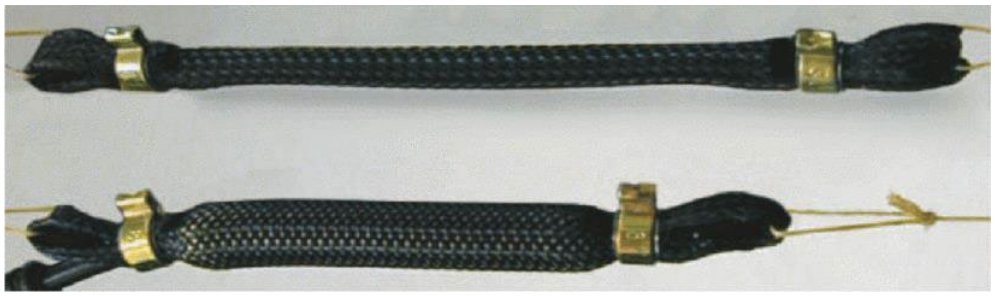

*Figure 10: Shortening Motion of Air Muscle, top is unactuated, bottom is actuated [20]*

### 1.4.2 Cable Driven Actuation

Cable driven actuation is a simple and robust way to manipulate robotic links. This system only requires use of cables, actuators, and a backbone structure for attaching and guiding cable. The driving cables are often attached to the driven links and passed through the structure to the near end of backbone, then connect to the actuator. When a cable is pulled by the actuator with force F, a bending moment M resulted to the robotic link calculated as equation (1) (Fig.11), therefore cause bending. Since the resulted bending angle $\alpha$ is entirely relied on effective cable length $\Delta L$, this method also has advantage in control precision. Cable selections could be anything from fishing cable for smaller scale robotic fingers [21], to steel cable for multiple meters long snake-arm robot (Fig.12) [22]. There are plenty of actuators selection of cable, small scale robotic arm is typically driven by linear actuators and servo motors, which will be

further explained in section 2.3.3. Due to the great amount of studies have done in cable driven actuation, this thesis will focus on a novel way to actuate the robotic arm.

$$M = F * d \quad (1)$$

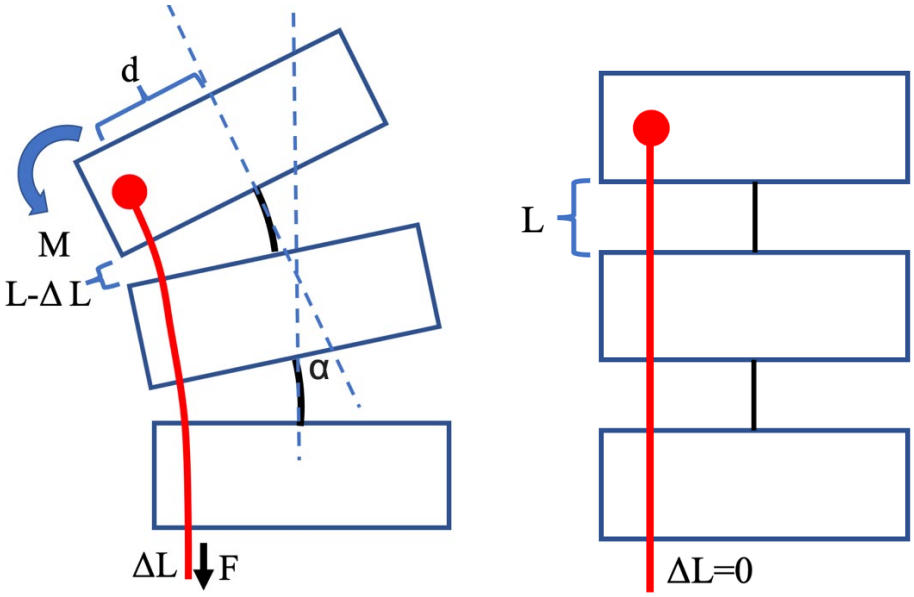


*Figure 11: Schematic of Cable Driven Continuum Robotic Arm*

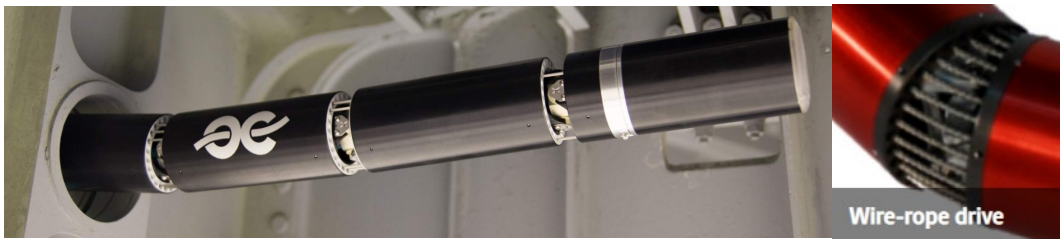


*Figure 12: Cable Driven Robotic Arm by OC Robotics [22]*

### 1.4.3 Compliant Rod Actuation

The mechanism of compliant rod driven actuation is similar to which with cables. As shown in figure 13, the rod (red) is attached to the tip section (blue) passing through the backbone and driven by a force (F). Since the actuating force is always tangent to the rod and perpendicular to the driven section, it causes a bending moment to the driven link very much alike cable

driven mechanism. The additional feature that rod driven actuation is capable of, by displacing just one rod the arm archives bending in both directions on a plane by pushing or pulling (fig.13). This allows the robot to accomplish more complex shaped by adding rods to the unused guidance channels and enhance the controllability of the robotic morphology. As shown in figure 14, a robotic link can form an "S" shape by pulling or pushing the rods simultaneously. This would be challenging for cable driven robots with the same amount of links.

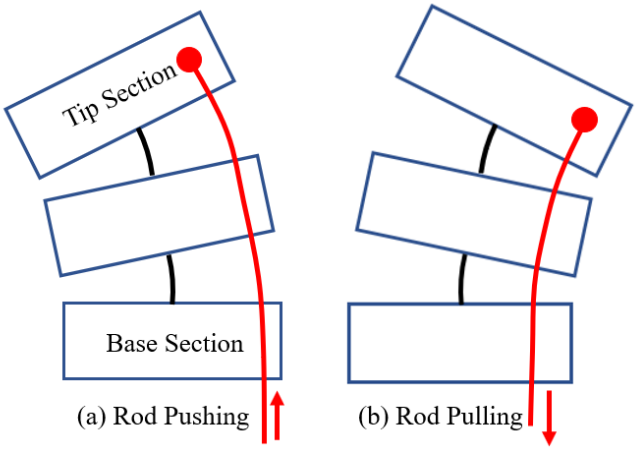


*Figure 13: Mechanism of Compliant Rod Driven Actuation*

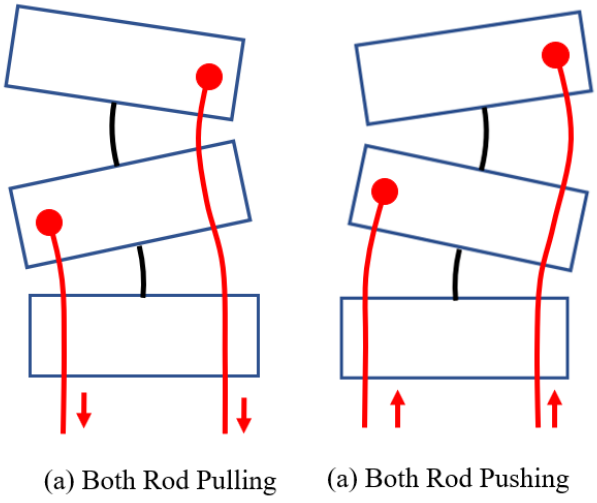


*Figure 14: Compliant Rod Driven Robot Bend in "S" Shape*

## 1.5 Thesis Objective

The early objective of the project is to study the current state of arts of compliant robotic arm design, various stiffness, and actuation methodologies. The main purpose of this thesis is to design and fabricate a functional prototype of a modular designed tubular shaped compliant robotic arm. The developed prototype will be capable of move from a starting point, and reach a given target position passing through multiple obstacles a in complex environment and, at this point, maintain its position steadily while carrying weight cooperating with variable stiffness technology.

## 1.6 Novelty of Thesis

Previous research has primarily focused on improving the control methods, like closed loop control [23], to overcome the shortcomings of compliant robots lacking accuracy and high payload carrying capability. This novel method, with the addition of variable stiffness and modification of the body structure, shores up the previously highlighted limitations of soft designs to a significant degree. In the future, this technology can be applied largely in minimal invasive surgery and complex mechanical system maintenance. The arm uses twin-pivoted backbone design to achieve a robust robotic arm with large inner space for wires, air tubes, and gadgets. An innovative actuation method using compliant rod and servo motor is also introduced in this thesis.

## 1.7 Overview of Thesis

This thesis is composed of five chapters. Chapter one introduces background study of each subject in the research project, including soft robots, variable stiffness technology, and backbone design of continuum robotic arms. This chapter also introduces different ways to realize variable stiffness, twin-pivoted backbone design for the tubular shaped robotic arm, multiple solutions for actuation, and their pros and cons comparison. The objectives and novelty of this research were also included in this chapter. Chapter two elaborates the entire design and manufacturing process of the prototype in detail, including the material selection, part fabrication, and final assembling. Chapter three documents the stiffness and workspace testing process from the experimental setup, testing procedures, to the result analysis. Chapter four concludes the research project and portray the potential future works.

## Chapter 2: Design & Prototyping of Robotic Arm

### 2.1 Tubular Shaped Backbone

The modular designed backbone contains 3 stages. Each stage is structured with a base, a connection link, 7 outer rings, and 7 inner rings. Figure (16) shows the front view of a robotic link assembled with an inner ring, an outer ring, and a clamp. The inner ring has an inner diameter of 17.5mm which leaves plenty of space to integrate sensors, wires of end effectors, and other gadgets. The four holes near the inner wall are for holding the compliant joints, with a diameter of 1.7mm which is 0.1mm larger than the diameter of joint rod. The other 16 holes are for guiding/attaching the actuation rods. They have a larger dimension of 2.0mm because multiple versions of prototype have shown that larger holes for driving rods can reduce actuation resistance, especially when pushing. This is because the driving rods bends during actuation against the inner wall of the guiding channel, resulting in elevated resistance for actuation. Theoretically, the guiding holes require colinear relationship when the backbone is straight, this is difficult to achieve with smaller guiding channels because all robotic links are assembled and aligned by hand. The larger diameter adds tolerance for aligning robotic links. The inner ring is fabricated using laser cutter for a smooth finish at the guiding channels and minimizes driving resistance (fig.15). The main function of the outer rings is to hold the inner bag. The purpose of having the groove is for clamping the inner bag steadily onto the backbone. Their outer diameter is reduced to a minimum to achieve a slender shape, thus having enhanced adaptability in complex environment, while maintaining all function of backbone and matches manufacturing capability at DISL. The outer ring is fabricated using 3D printer. Inside the base section, there is an integrated air channel designed for the air tube to pass through from the inner layer jamming bag to the air pump behind the dock (fig.17). The channel is designed to

tilt 45 degrees to attach to the bag for reducing the turning angle it needs to make inside the base. It also provides a larger contacting area for a better adhesive quality. The air tube at the later stage can pass through the air channel designed in the connection link and utilized the cavity created by the tubular backbone, then connect to the air pump.

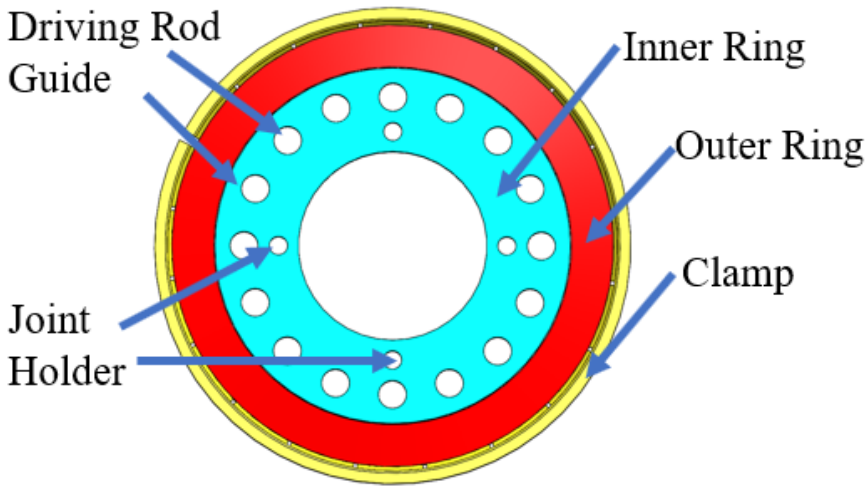


(a)

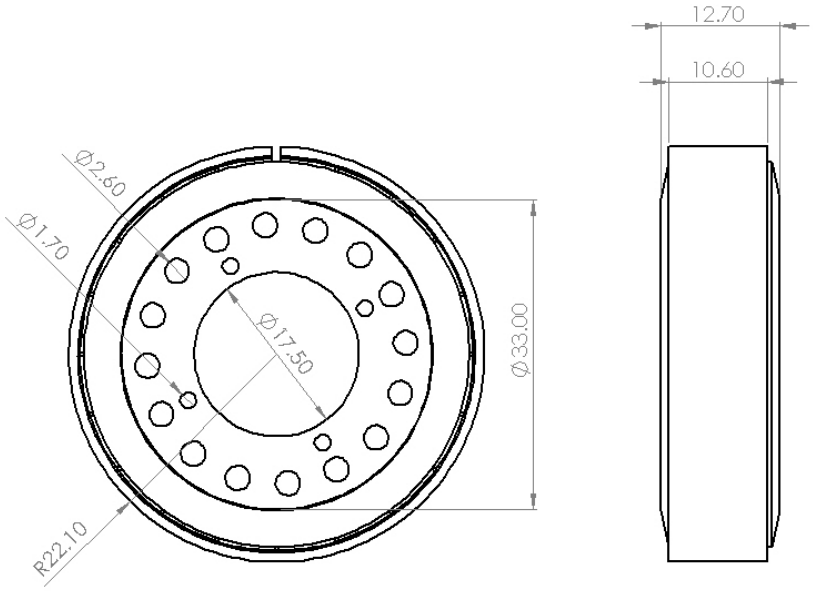


(b)

*Figure 15: (a) Front View of a Robotic Link Assembly (b)Robotic link Assembly Dimensions*

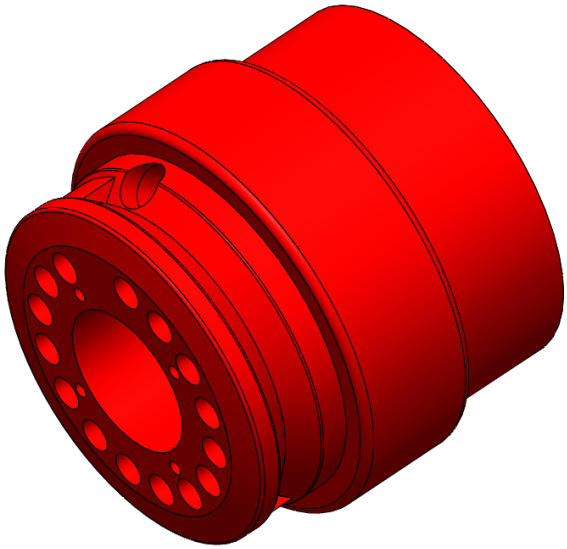

(a)

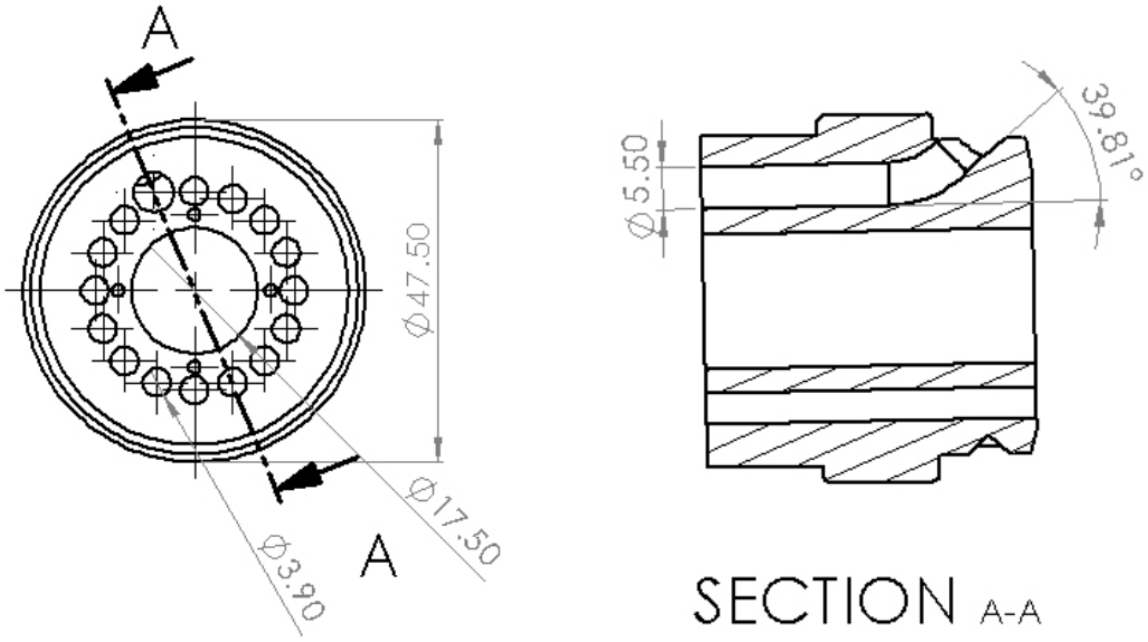


(a) (b)

*Figure 16: Base Section (a) Isometric View (b) Back View (c) Cross Section View*

The first stage of the continuum robotic arm prototype has a base section for connecting to a dock for testing and future mobility purposes. At the later stages the base link is replaced with connection links for mounted to the early stage. This link makes the novel modular design of the prototype possible. The backbone is assembled in the pattern as shown in figure 18. The gap between every two robotic links is crucial since they determine the maximum bending angle of the arm, as well as whether buckling of actuation rod would occur. All compliant joint rods are laser cut to mm in length so with the two ends fully inserted and glued to the robotic links, the gap in between is left to be 30mm. The gap length was proved by testing that would not buckle during actuation.

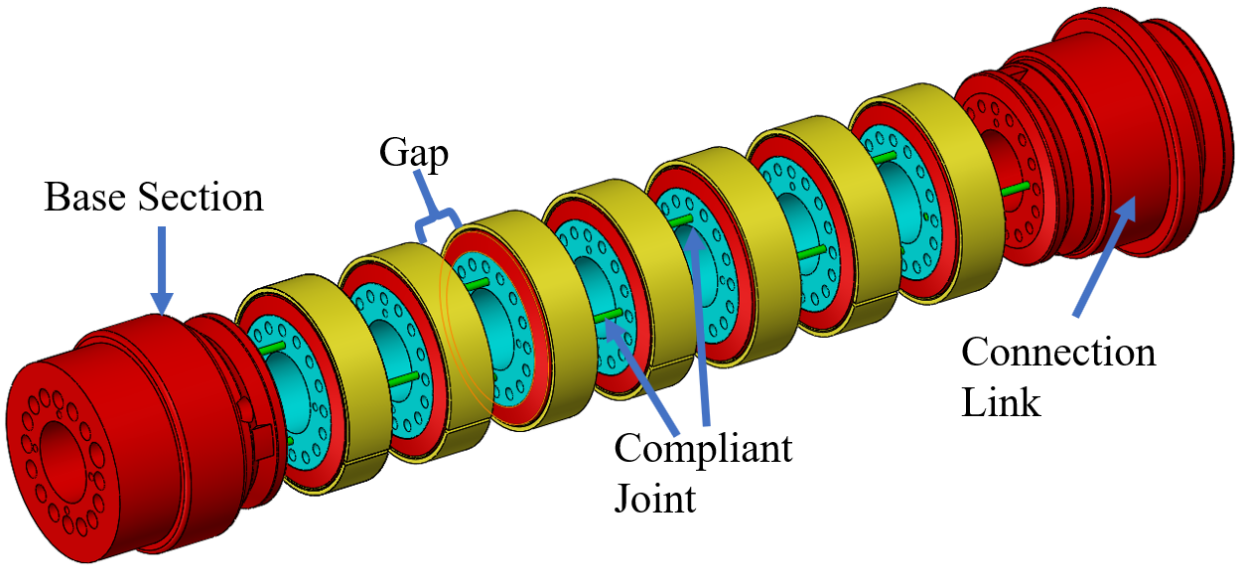


*Figure 17: Isometric View of Robotic Arm Prototype Stage 1*

The prototype in this thesis is modular designed to have multiple stages that can be added to the robotic arm for serving in different applications. The connection link is a key component of this design. It has a structure that can be clamped with the adjacent stage (fig.19). The clamp was 3D printed with heat sinks installed for screw tightening. The actuation rods attached to

the later stage arm is guided to pass through the early stage and connect to the actuator. To prevent interference of the actuation rods, the later stage arm rotates 22.5 degrees angle so they can use the empty guiding channels. This prototype supports up to 3 stages of robotic backbone, with a total length of 600mm. The design significantly enlarges the workspace of the robotic arm.

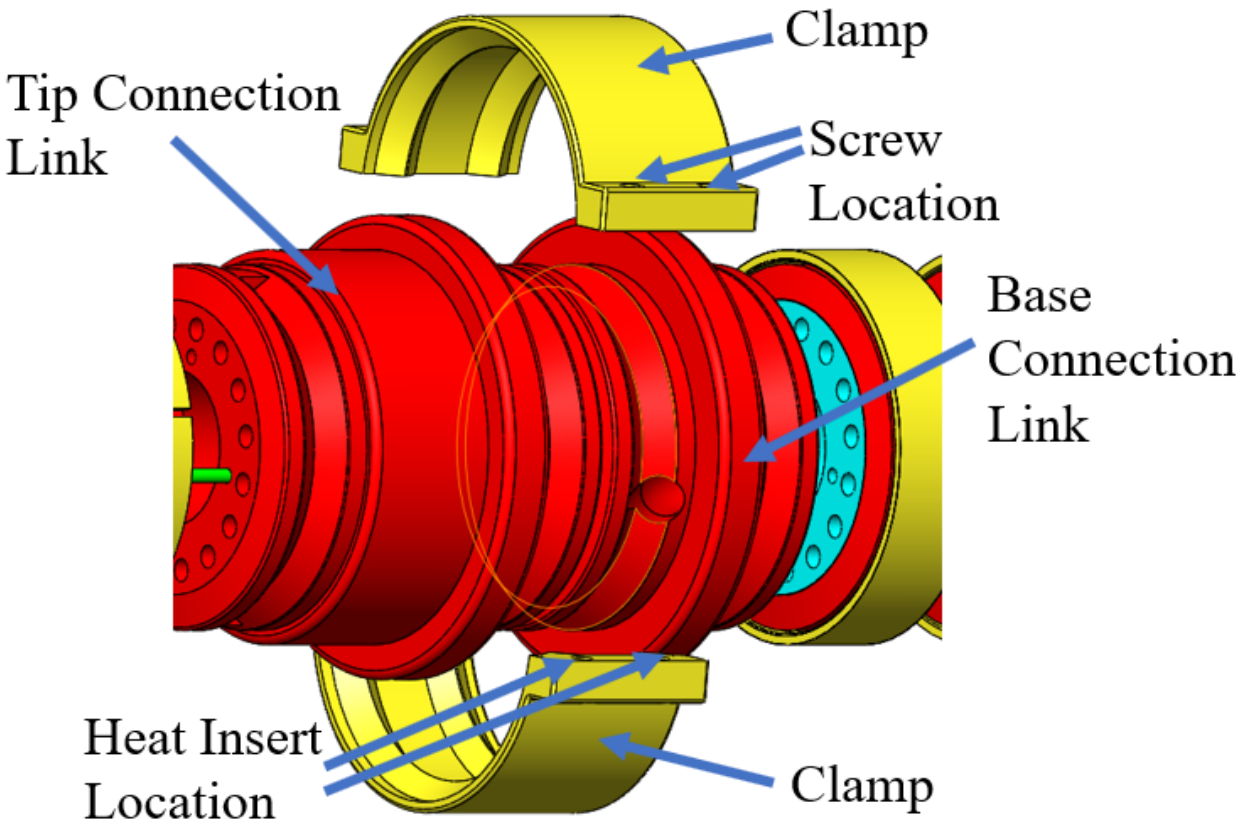


*Figure 18: Exploded View of Connecting Mechanism for Modular Design*

### 3.2 Layer Jamming for Variable Stiffness

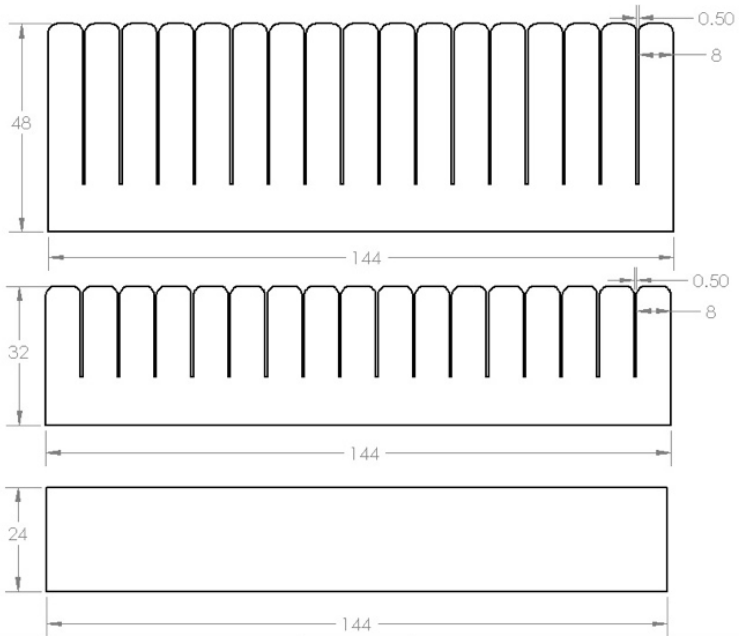


*Figure 19: Layer Design Drawing*

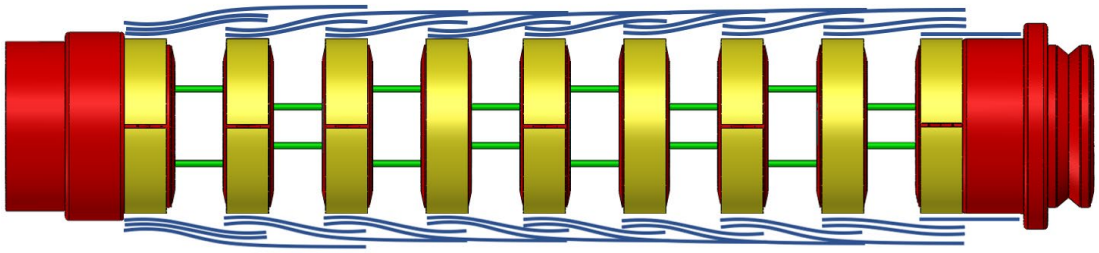

(a)

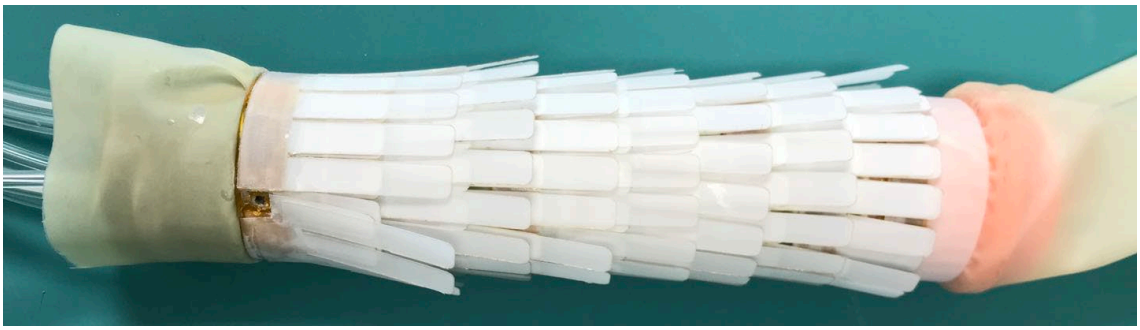

(b)

*Figure 20: Layer Layout for Stage 1 Prototype (a)Schematic of Layer Layout (b)Prototype with Inner Bag & Layers Installed*

For layer jamming variable stiffness function, polyester films were chosen for making the layers. This film was selected because their low friction at zero pressure, and when the vacuum pressure applies, the resulted friction force increases dramatically. All layers were designed in a similar way. As shown in figure 20, they are structured with a base of 11*144 mm, which correspond to the width and perimeter of the clamp for maximum adhesive contacting area. The layer strips with an equal width of 8mm was selected after trying multiple dimension, and the gap of 0.5mm was cut out to prevent layer interference. There are three versions of layers distinguished by their strip length, 48mm, 32mm, and a 24*144mm base which the only version with no strip. The 48mm long version covers three robotic links and two gaps, the 32mm short version covers two robotic links and one gap, and the base only version fully covers the connection link at the tip of every stage. These three versions of layer ensure three overlapped layers on every gap at all time. This is significant for maintaining a constant stiffness across the entire robotic arm. When every gap is covered by overlapped layers with equal contacting area, the friction force constraining every adjacent two robotic links are equal, thus results in constant stiffness at everywhere. Different number of overlapping layers can lead to uneven stiffness, eventually reduce the overall stiffness of the arm. Figure 21 shows the layout design of the layers on one stage of prototype. The layers are fabricated with a laser cutter. It can cut through the polyester films quickly and precisely.

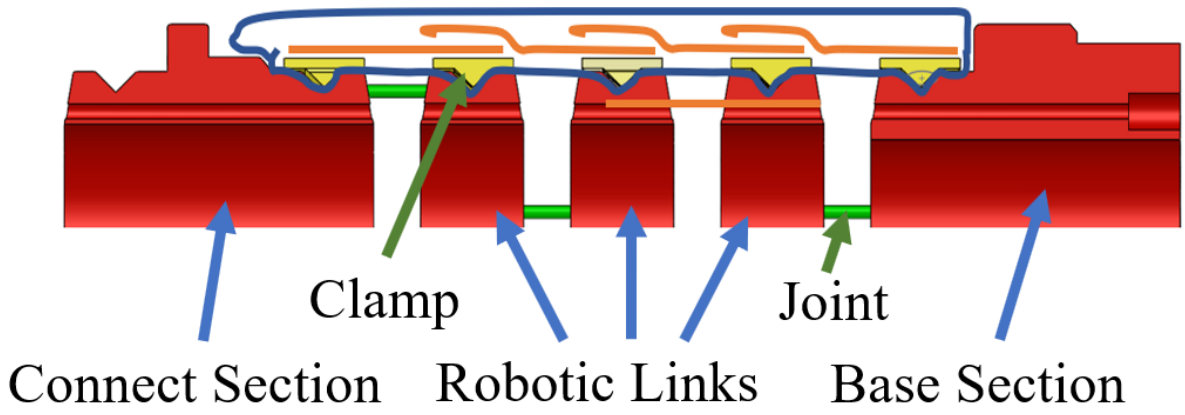


*Figure 21: Simplified Schematic of Vacuum Bag Layout Design*

A sealed bag is another significant parameter of layer jamming variable stiffness feature. It is important to have a well-sealed bag. When a vacuum pressure is applied, the bag presses onto the friction layers. With this normal pressure the friction force constraint is generated. The expectations for bag material and layout are:

- Low friction when contacting with layers
- Airtight
- Minimum cavity
- Doesn't prevent arm's motion

According to these requirements, 0.4 mm thick latex membrane was chosen for layer jamming bag fabrication, with a backbone outer ring and clamp was specifically designed for layer jamming bag layout. Figure 22 shows a simplified version of the layer jamming bag layout. The enclosed blue line indicates the latex bag, the oranges lines represents the layers, while the other parts are cross section view of half of the robotic arm backbone. In this bag layout design, both inner and outer part of bag enwrap the outside of backbone. Inner bag covers the

outer ring and fixed by the clamp. Above the clamp is friction layer is glued to the clamp by super glue. Finally, the outer bag covers all layers and glued to inner bag. This bag layout encloses all layer jamming structures with minimum cavity at zero vacuum pressure. This reduces the time to achieve high stiffness to a fraction of a second. In addition, it's very efficient in terms of bag material usage and adhesive needed boundary length, which lower the risk of air leak. An integrated air channel was also designed to cooperate with the bag layout, minimizing the wear of bag-tube adhesive while maintaining a clean appearance. Attached to the inner bag is an air tube that goes through an air channel integrated in the base/connection link (Chapter 3.1), then utilize the inner space of the tubular shaped backbone and connect to the air pump. Figure 23 shows layer jamming effecting on stage 1 of robotic arm prototype. On the lower left corner of the figures is a Mark X gauge showing the encountered force at the tip of the backbone. Figure (a) shows the initial position which the force reading is zero, figure (b) shows the prototype can only handle 1.26N at 0 psi, and figure (c) shows the prototype handles 13.4N when layer jamming is functioning.

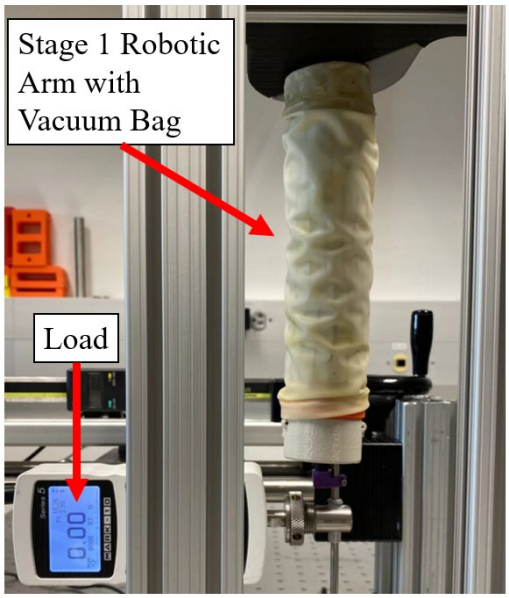


(a)

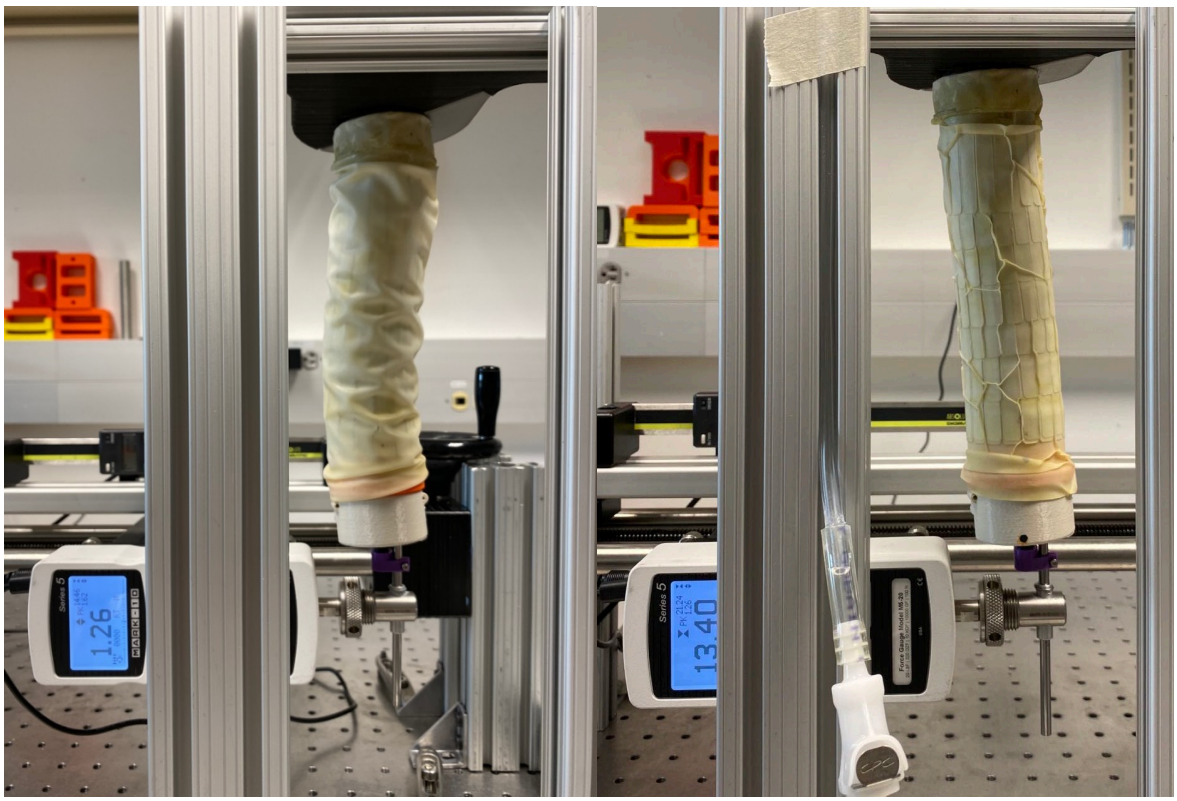


(b) (c)

*Figure 22: Layer Jamming Function Testing*

### 3.3 Compliant Rod Actuation

Compliant rod actuation is setup similarly as that of cable actuation. As shown in figure (), there are four rods attached to each backbone stage. Rod 1 and 2 connect to the connection link at the furthest end of the backbone, while rod 3 and 4 are attached to the fifth link which is in the middle of the backbone. Rod 1 and 4 controls the robotic arm to bend about y-axis, while rod 2 and 3 controls the robotic arm to bend in about x-axis. Since each stage of backbone contains 8 equal gaps, rod 3 and 4 can actuate the arm to a half of the maximum bending angle. The displacement of rods is directly related to the bending angle of the backbone. When rod 1 or 2 is pushed or pulled by 32mm, the robotic arm reaches its maximum bending angle of 86 degrees. The bending angle can be approximated by mapping the displacement of 0 to 8mm to

0 to 86degrees. The actuation displacement has a relationship with the bending angle where $x = 32 - 8 * \left(\frac{8}{\theta_{rad}} - 22\right) * sin\frac{\theta_{rad}}{2}$ mm (fig.26). By inputting the designated bending angle $\theta$, the needed displacement of x can be obtained. The prototype can bend in any direction in a space by actuating both rods attached to the same robotic link, by combing the bending motion in the two perpendicular planes. The robotic arm can also bend into an "S" shape by actuating rod 1&3 or 2&4 in the same direction. This further enhances the workspace of the robotic arm prototype.

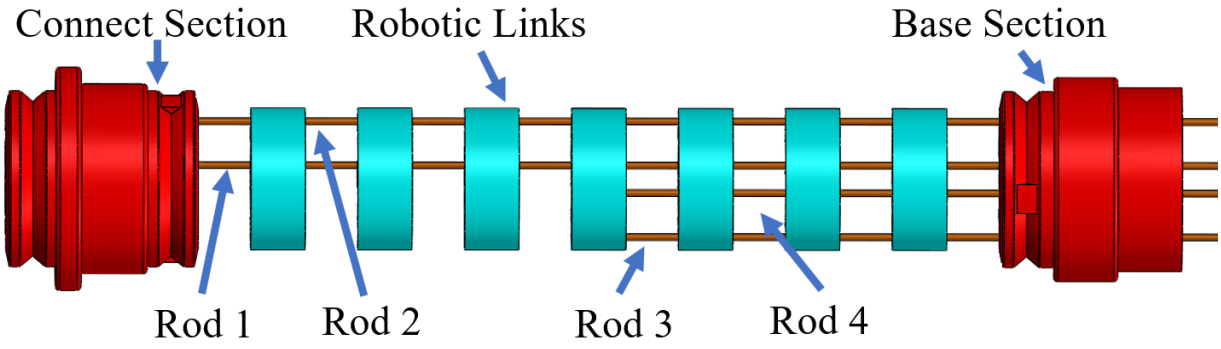


*Figure 23: Rod Layout Schematic of Stage 1 Prototype*

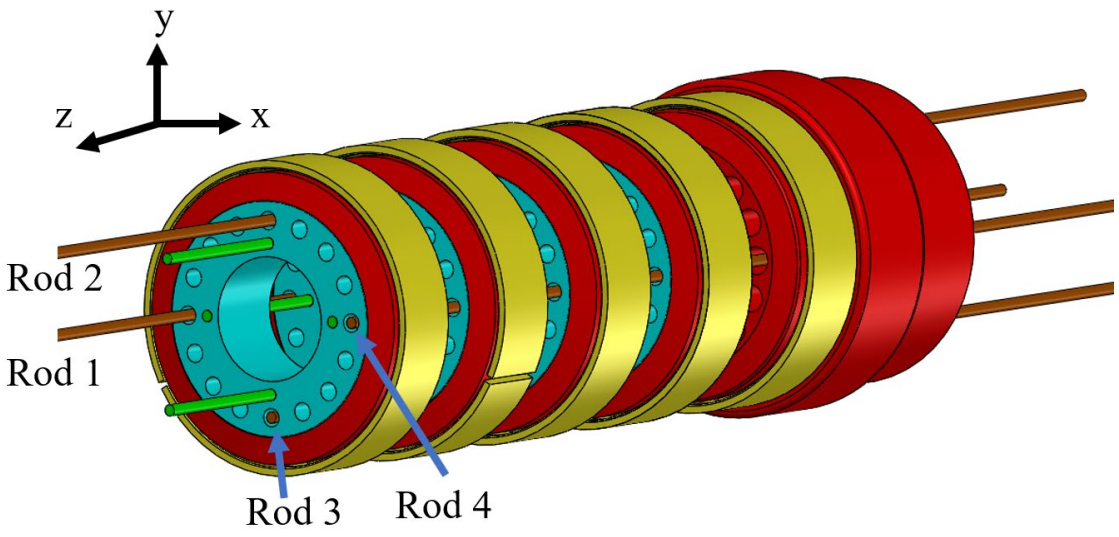


*Figure 24: Isometric View of fifth Link to Base Section*

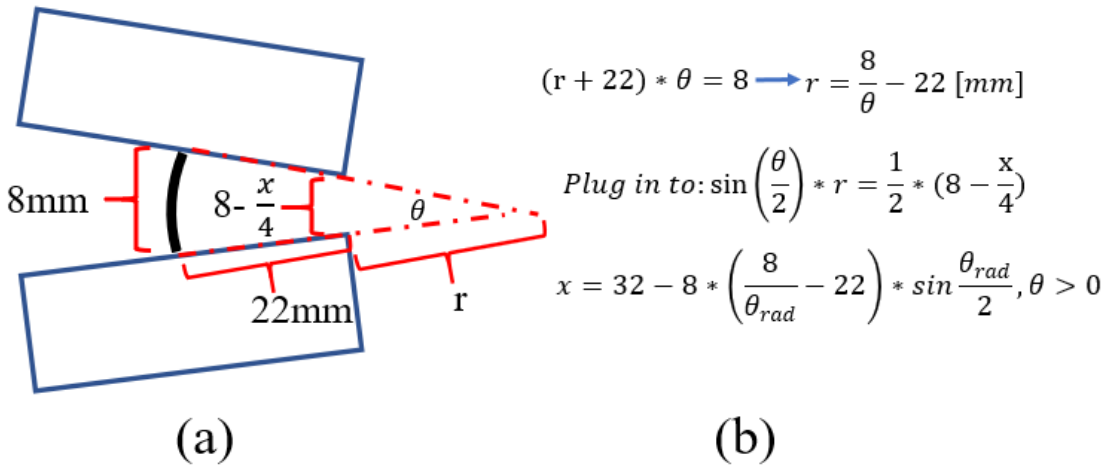


*Figure 25: Calculation of Bending Angle in terms of Actuation Length*

Both cable and compliant rod need actuators to drive to achieve bending. In the prior studies linear actuator is the most commonly used actuator for cables. They have advantage of high actuating force and precision. However, its mechanism constrains the motion of robot when not actuated. This adds stiffness to the robot at soft state. Additionally, they are expensive considering this thesis requires 4 actuators to drive each stage of robot, and up to 12 actuators for the entire prototype with 3 stages. Previous study in DISL have shown horn-equipped servo motor can drive cables with a superior performance. This thesis designed a similar mechanism to actuate the robotic arm prototype. Figure 28 shows the actuation box design cooperating the servo driven compliant rod actuation method. The grey parts are the main body of the actuation box made of acrylic boards with laser cuter. The Red part is a servo bracket since the selected servo does not contain any mounting wings. The servo bracket is 3D printed with heat sinks and screws installed for mounting onto the actuation box with a high clamping force. The actuation box contains a pin-in-slot mechanism to drive the fixed joint on rod and cause displacement. The boards on left and right of the box are for holding the aluminum tubes, which constrains the motion of the rigid actuation rod. A copper part is used for fixing the rod

and sliding in the slot of servo horn (fig.29). As shown in figure 27, when the servo stays at position 1, the arm is controlled to be straight. When it rotates to position 2, the servo horn drags the fixed pin on the rod and pull the rod to the left. While the servo rotates to position 3, the rod is being pushed to the right. Then the resulted displacement converts to bending angle of the prototype. The maximum displacement is 35mm as each stage of prototype requires 32mm of travel to reach maximum bending. The servo arm is designed to 40mm long with the distance between the end of slot to the center of rotation be 35mm, so the arm is able to drive the rod to its designed maximum position with 60 degrees of rotation. The relationship between servo rotation angle and rod displacement is $\theta = \tan^{-1}\frac{d}{17.5}$

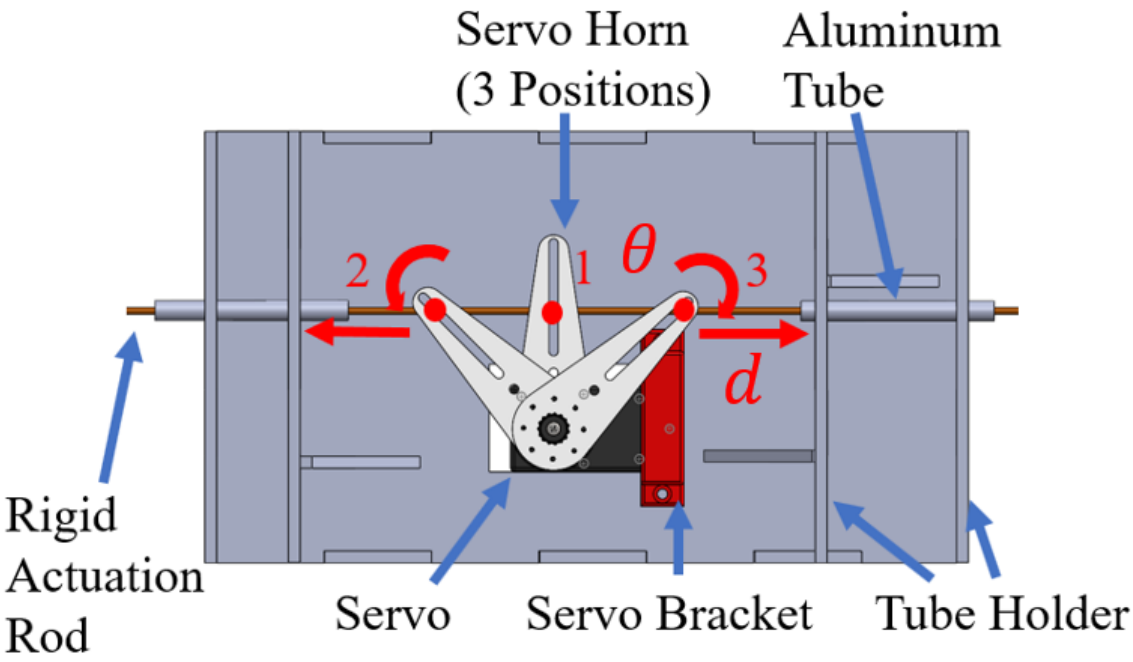


*Figure 26: Top View of Actuation Box with Servo Horn in 3 Positions*

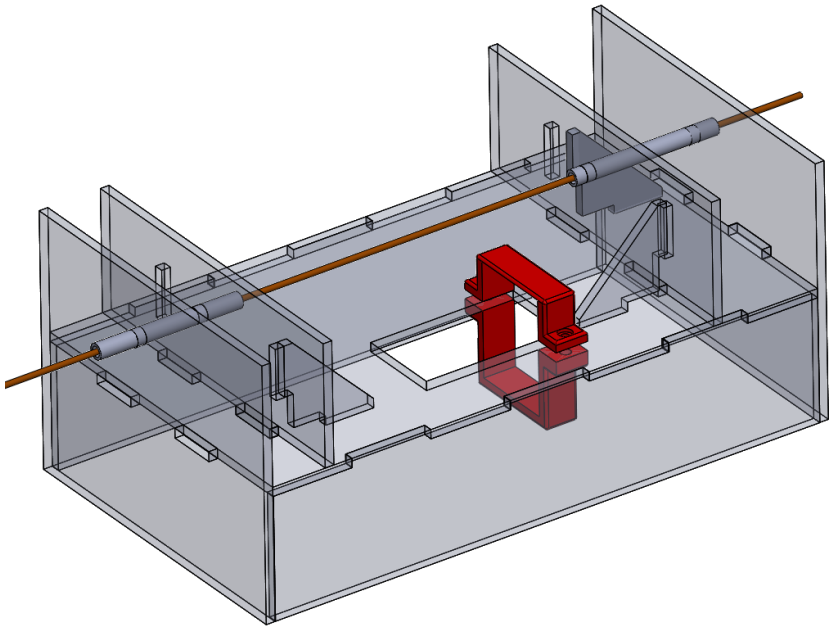

*Figure 27: Isometric View of Actuation Box (without Servo Motor)*

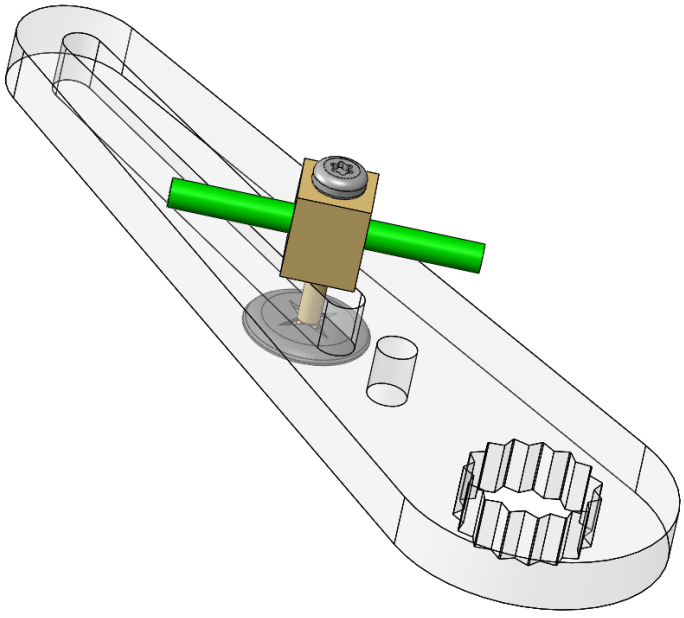

*Figure 28: Assembly of Pin Slider, Rigid Driving Rod, and Servo Horn*

Daran A15-ST servo motor was selected in this thesis. It is compatible with Arduino control board, with torque capability of 15kg*cm, maximum speed of 0.25 seconds per 60-degree-rotation, capability of rotating 270 degrees and working voltage of 7.4V. It has 4 modes: Standby, damper, lock, and wheel. This prototype uses the standby mode for rotation and wheel mode while the other servos are working. Rotary encoders are used for controlling the servo motors rotating to different positions. By manipulating the encoder clockwise or counterclockwise, it controls the servo to drive the robotic arm to achieve different bending angles.

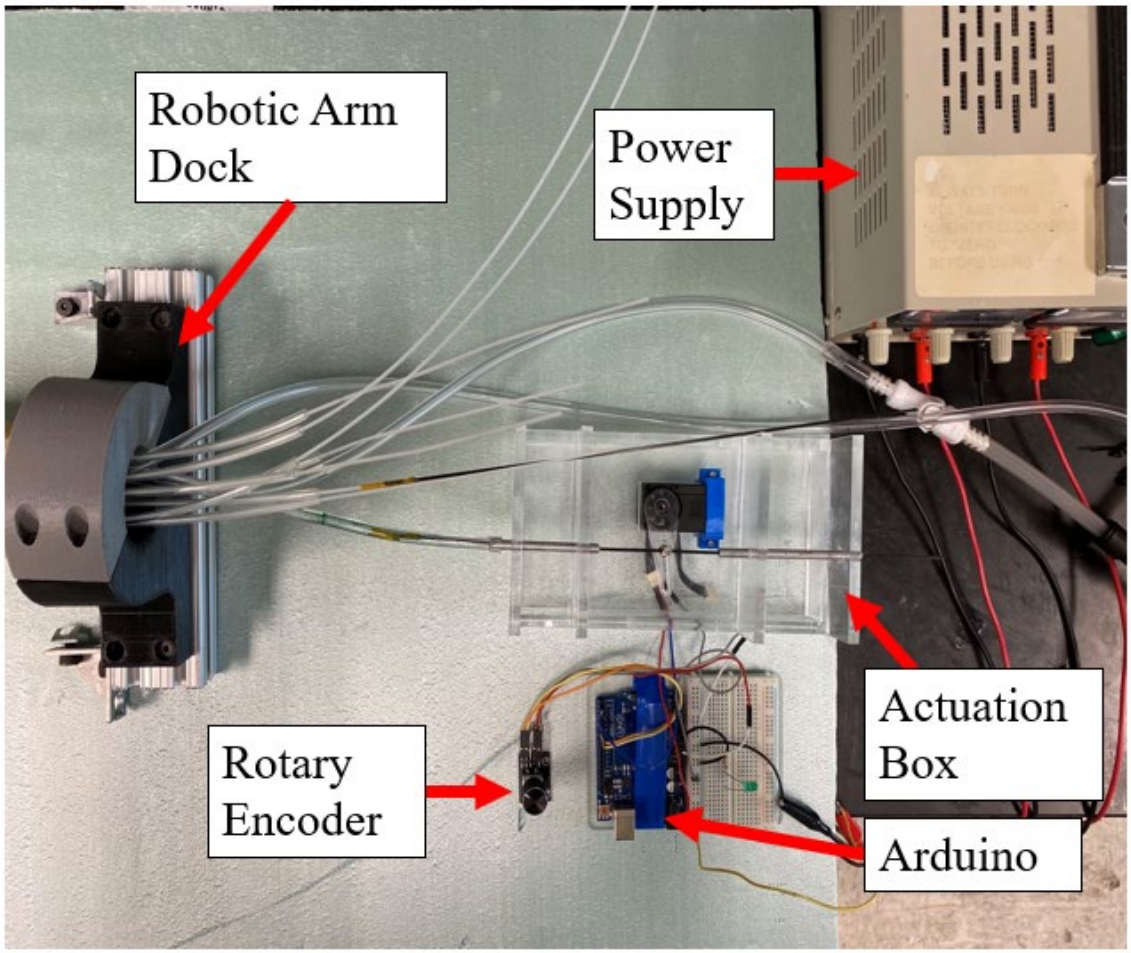


*Figure 29: Actuation System Setup*

### 3.4 Fabrication Process of Prototype

The fabrication of prototype starts with the backbone, since it holds all other components. While the outer ring links, connection links, and base links are 3D printed, the inner rings and compliant joint rods were laser cut to a precise dimension(fig.31). Super glue was used to assemble the backbone models for light weight and strength.

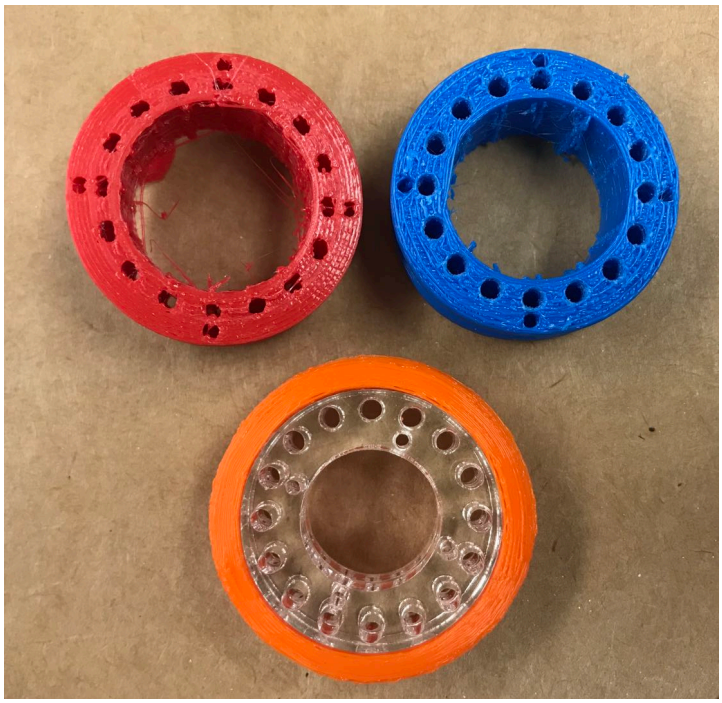

*Figure 30: Comparison of surface finish in 3D Printed Robotic link (upper) and Laser Cut/3D Print Combined Robotic Link (Lower)*

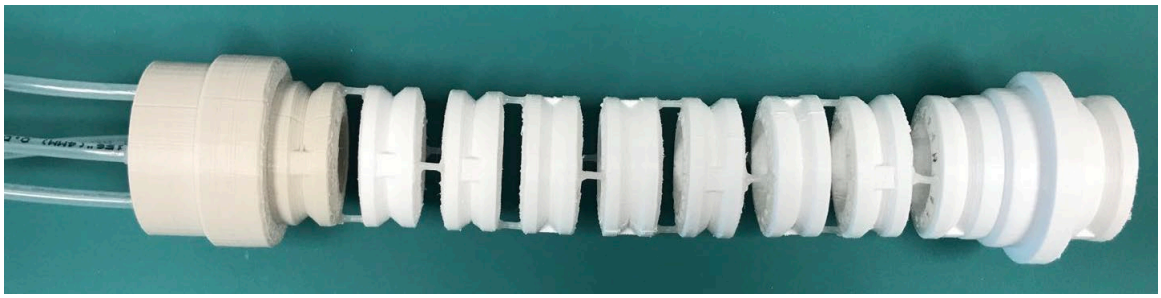

(a)

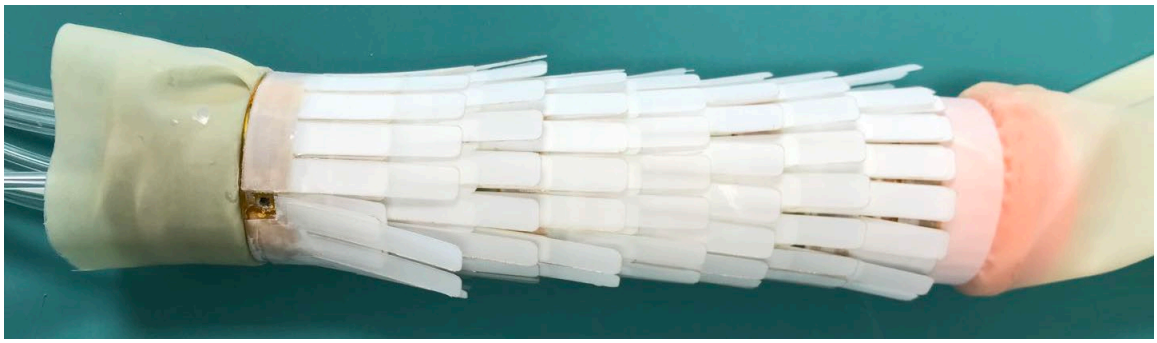

(b)

*Figure 31: Fabrication of (a)Backbone (b)Layer Jamming Components*

Layer jamming structures are prepared by 3D printing the clamps, laser cutting the polyester sheets, hand cutting a sheet of latex membrane with twice length of backbone, and width of outer diameter of robotic arm. The bag is fabricated by cohering latex membrane to a tube using rubber cement, which maintains the compliancy of membrane after coherence. After attaching an air tube to the bag at 45 degrees angle using glue, the bag was enwrapped to the backbone and fixed with clamps with air tube fitted into the air channel. High strength tape was used for tightening the clamps and prevent movement of layer, which was attached onto the clamps with super glue（fig.31). Finally, the entrance of air tube was cut open and the bag was closed. To fabricate the actuation box, acrylic boards are laser cut to the designated dimensions and assembled together with super glue. The servo bracket is 3D printed and bolt onto the box using heat inserts and screws. The rigid driving rods, which in this thesis are 1.6mm diameter carbon fiber rods, are attached to the compliant actuation rods using metallic tape and super glue (fig.32). This tape has advantage of high strength and it is untraceable, so it does not shred during the rod is pulled. Super glue was used for reinforcement. Then the servo arm is attached to the carbon fiber rod with the pin slider. In the final assembly, the air

tube from robotic arm with the aluminum tube is included in the actuation system to achieve the final prototype(fig.33).

*Figure 32: Carbon - Nylon rod attachment.*

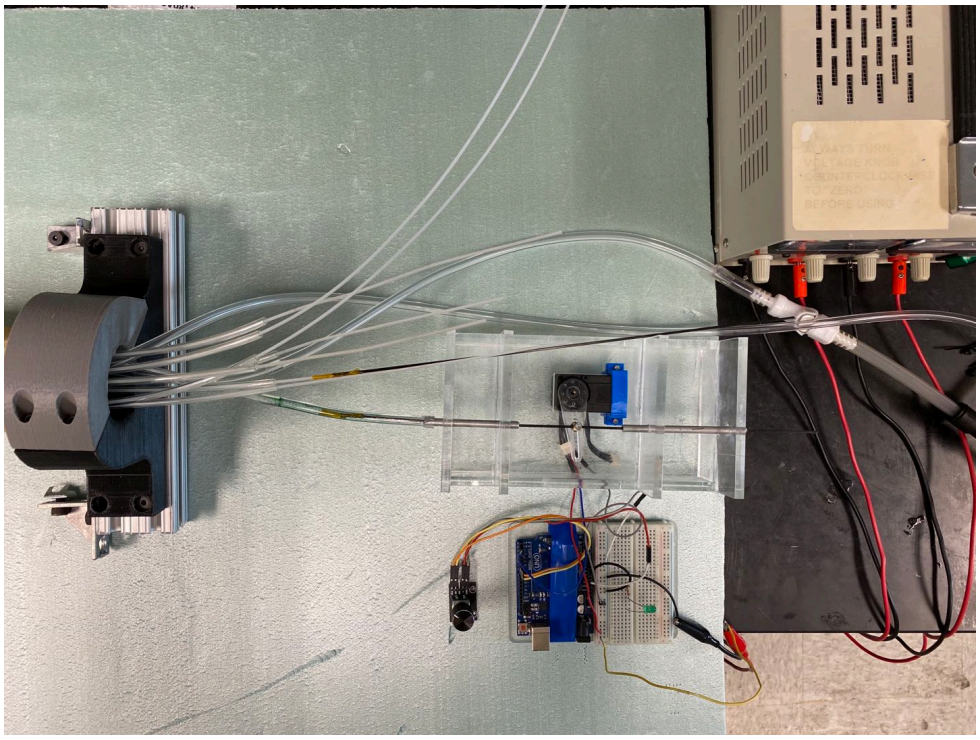

(a)

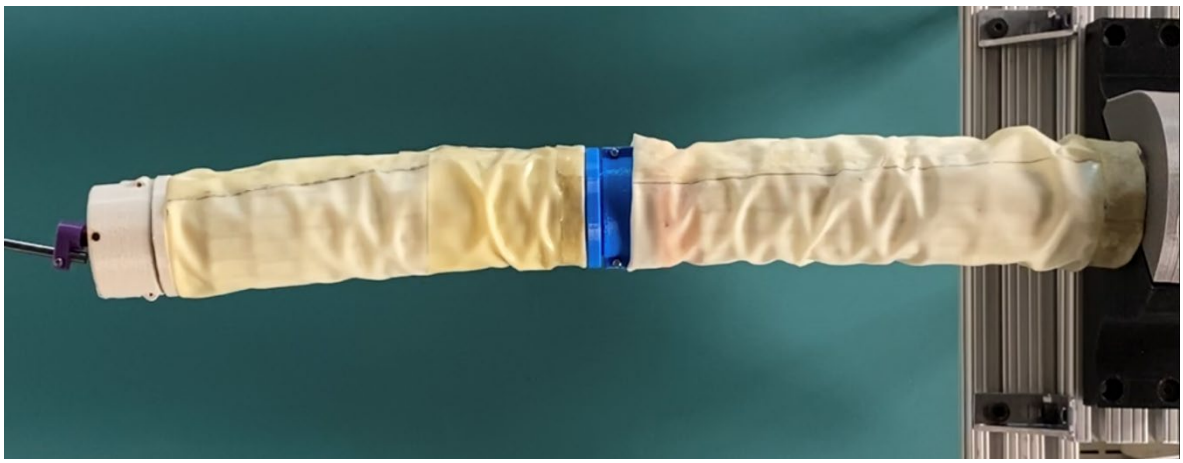

(b)

*Figure 33: Final Prototype (a)Actuation system (b) 2 stage Robotic Arm*

# Chapter 3: Testing & Results

## 4.1 Stiffness Test

A stiffness test was performed to examine the effectiveness of layer jamming variable stiffness function. In this test, the robotic arm prototype was mounted vertically with the tip pointing down to eliminate the effect of gravity to the data results. The test records the load of the prototype can handle at the tip at different positions. As shown in figure 34, the test setup includes a Mark X force Gauge and a displacement gauge mounted to a testing frame, while the robotic arm prototype was fixed to another aluminum frame pointing. An adapter (fig.35) was made for connecting the tip of the prototype to the Mark X force gauge. This mechanism ensures accurate force measurement by preventing prototype slippage from the sensor. The test was performed by pushing the tip of prototype in x axis from 0 to 20mm displacement with an increment of 0.5mm. Each data point was recorded after a pause of 5 seconds to let the robotic arm stiffness stabilize. Data recording stops after retrieving tip displacement and force gauge reducing to 0N. The testing results are shown in figure 36, with displacement being x-axis, and force being y-axis.

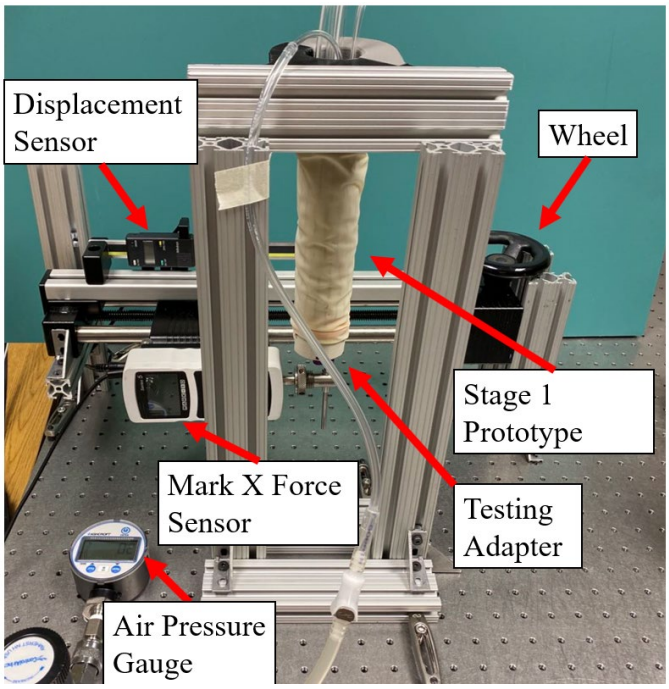


*Figure 34: Experimental Setup of Stiffness Test*

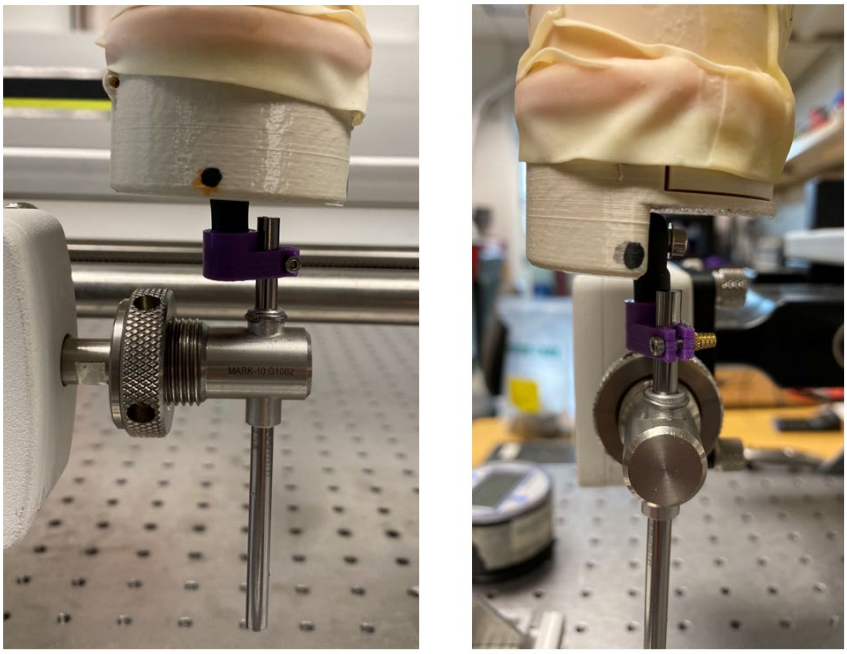

*Figure 35: Adapter for Stiffness Test*

The stiffness is calculated to be the slope of a fitted line at the beginning portion of the graphs:

$$\mathrm{E}_{0\mathrm{psi}} = \frac{y2 - y1}{x2 - x1}$$

Test results for stage 1 prototype show that stiffness increases as the vacuum pressure increases. For stage 1 prototype, the maximum stiffness of 1.5021N/mm occurs at 12.5psi, comparing to the stiffness of 0.01314N/mm at 0psi. With the addition of layer jamming technology, the stiffness of stage 1 prototype can increase as much as 114 times. Test results (fig.37) maintains the same trend for stage 1&2 prototype, except at 12.5psi, the stiffness is slightly lower than that of 10 psi. This could be caused a small leakage the stage 2 prototype, so that it can only maintain a vacuum pressure of 11psi. The stiffness for stage 1&2 prototype is smaller than which for stage 1 prototype. This could be caused by constrained air flow rate, due to the size of air tube and performance of vacuum generator.

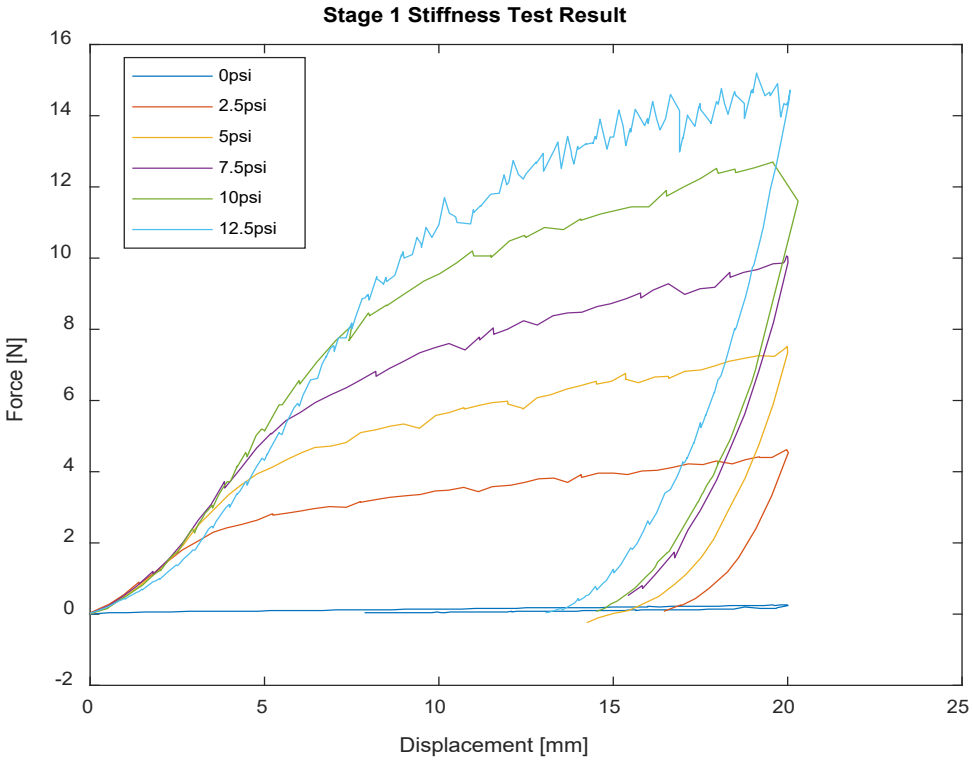


*Figure 36: Stiffness Test Result of Stage 1 Prototype*

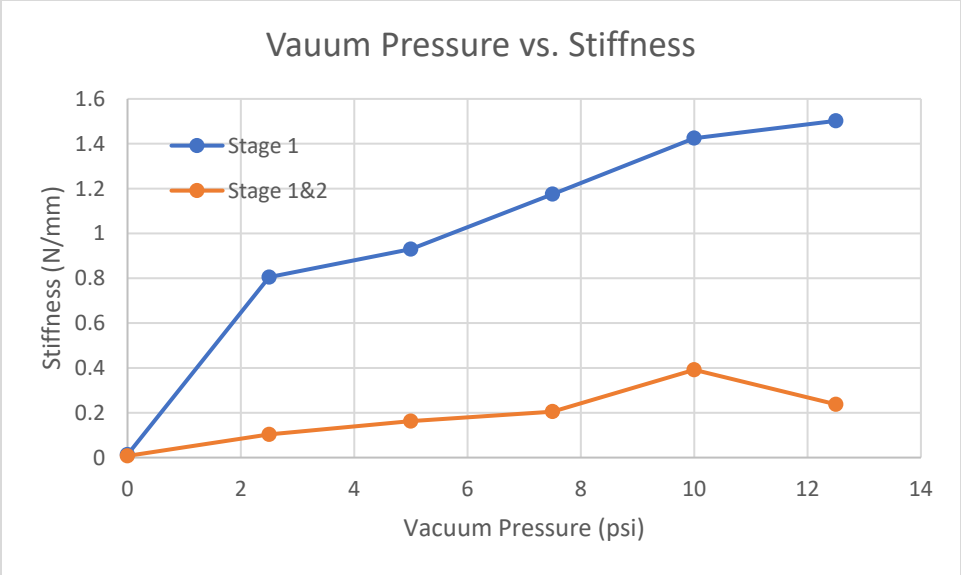


*Figure 37: Stiffness Result of Prototype with Increasing Vacuum Pressure*

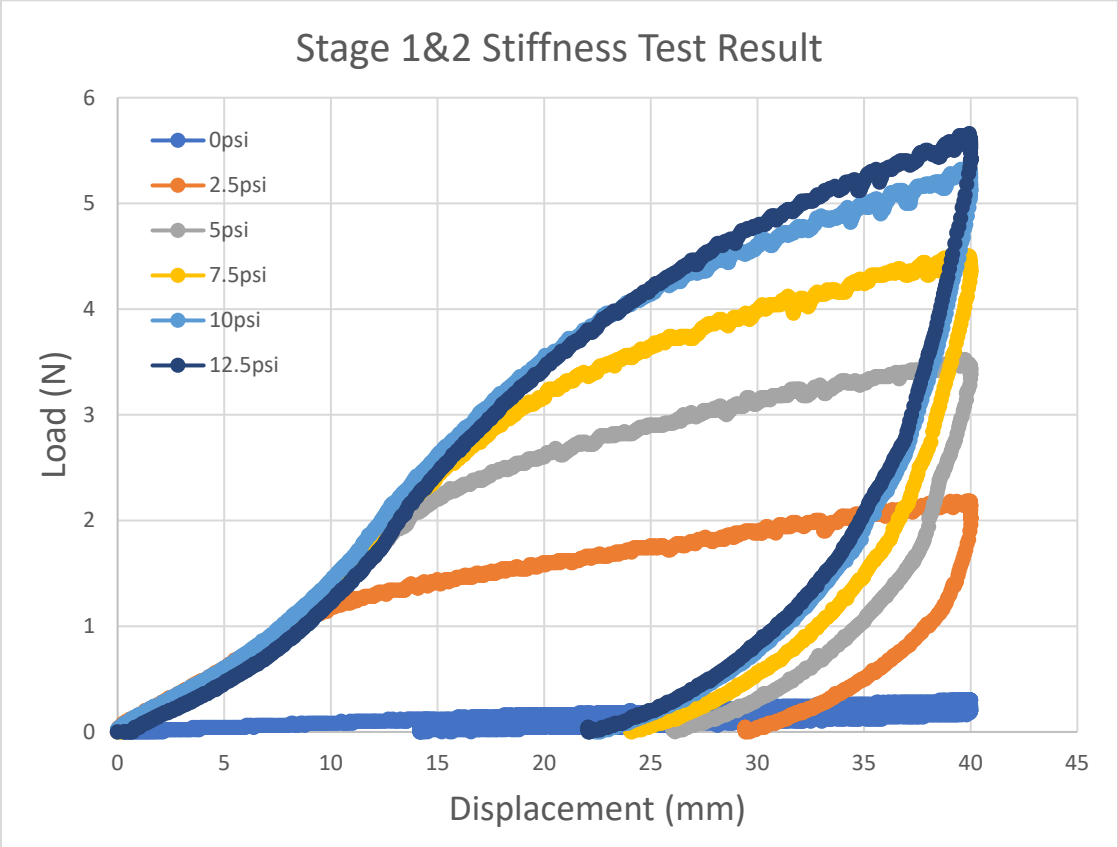


*Figure 38: Stiffness Test Result of Stage 1&2 Prototype*

### 4.2 Workspace Test

A workspace test was performed to examine the flexibility of the continuum robot prototype. In this test, the prototype was mounted vertically with the tip pointing down, a camera was set steadily to record the prototype perform bending in different directions. Then the video record was analyzed using Tracker App. This program tracks the position of a marked dot at the tip of the robotic arm. The coordinate system was set as shown in figure 39 with the origin locates at the near end of arm, and the arm length of 200mm was entered to the program. The result (fig.40) shows the 3D workspace from front of stage 1 prototype. It can achieve a maximum x position of ±125mm, and the maximum bending angle was measured to be 75.39 degrees for actuating by hand and 59.5 degrees for actuating by compliant rod. These values are smaller than the theoretical value of 86 degrees. This can be caused by 3 factors: Errors can be made in fabrication process that the dimension of complaint joint and robotic links are not exact, shorter joint length can cause smaller bending angle; Layer interference can prevent motion of robotic arm; Insufficient actuation is possibly due to the invisibility of joints; the operator cannot clearly identify whether a maximum bending has reached. Although the actuation rod is compliant, it still has a rigidity that increases the actuation force toward the end actuation, which results in a smaller rod actuation workspace.

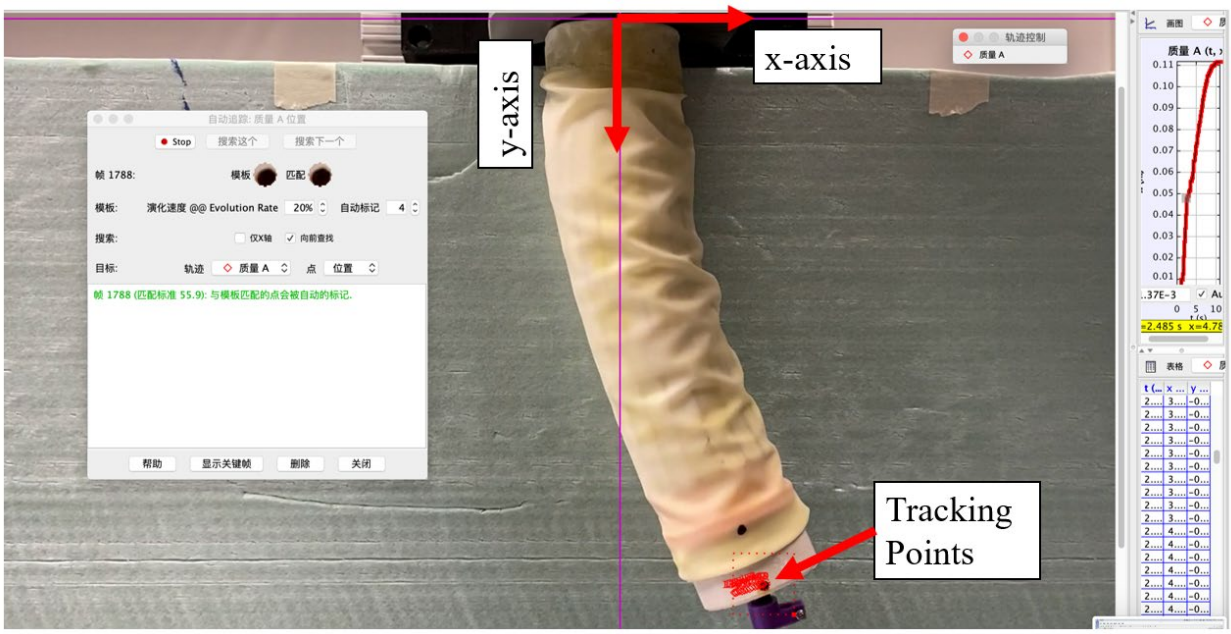


*Figure 39: Analyzing Workspace of Stage 1 Prototype Using Tracker app*

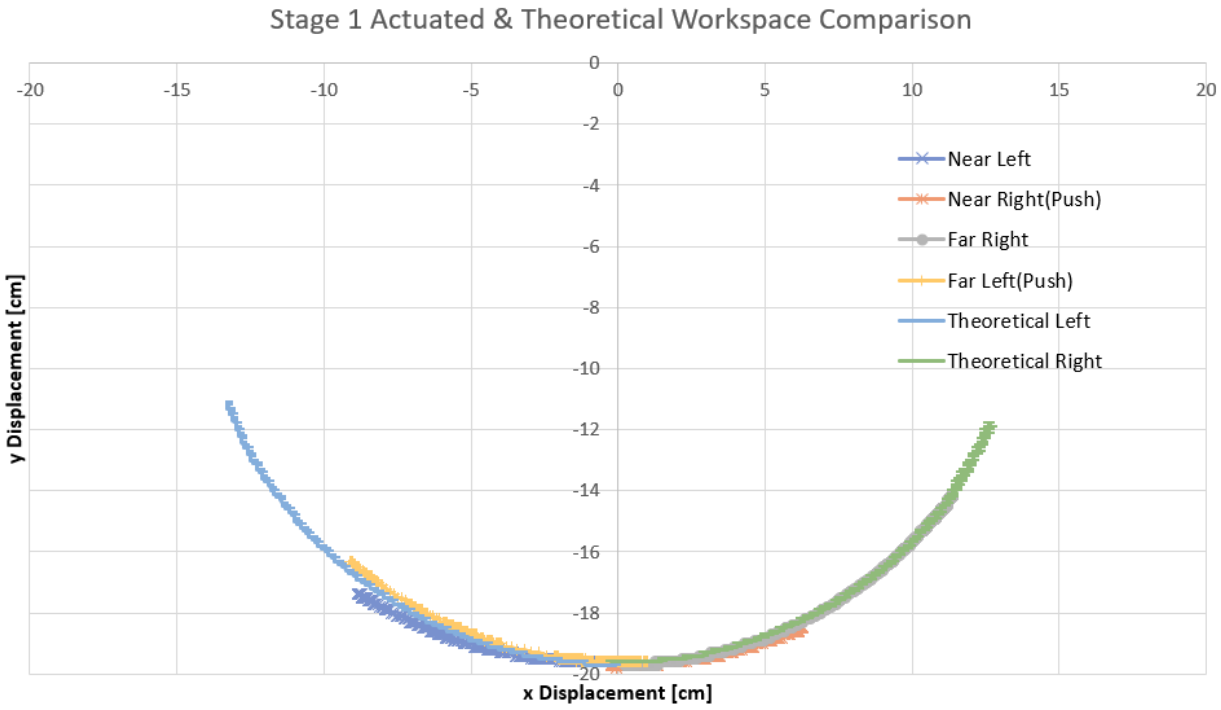


*Figure 40: Workspace Result of Stage 1 Prototype*

# Chapter 4: Conclusion

## 5.1 Summary

The objective of this undergraduate honors research project is to develop a working prototype of a tubular shaped continuum robotic arm with variable stiffness. The main goal is to integrate the benefits of conventional rigid robots and soft robots, also to attempt a novel actuation method. To achieve this, literature studies was done in multiple approaches of backbone design, variable stiffness function and actuation of continuum robotic arms. From the studies, strip shaped layer jamming was selected for accomplish variable stiffness, a twin pivoted design was determined for the robotic backbone prototype cooperating with a servo driven compliant rod actuation. A 2-stage modular continuum robotic arm was designed and built with 3D printed and laser cut parts. A stiffness test was conducted with a result shows 114 times of stiffness change can be made by 1-stage robotic arm and 32 times for 2-stage. A workspace test was performed and determined the 1-stage prototype able to achieve 75 degrees of bending and 150 degrees for 2-stage. The final prototype was able to bypass the obstacles and reach the target position in compliant mode, work accurately, and handle elevated payload in stiff mode. The main goal this research project was achieved.

## 5.2 Future Works

The stiffness of the prototype has an increasing relationship with the vacuum pressure, except the test result of stage 1&2 in 12.5psi. Indeed, the stage 2 prototype has a small leakage that can only maintain 11.3psi vacuum pressure, but this should still provide a higher stiffness than which in 10psi. This error needs to be studied in the future. The servo driven actuation box shows a drawback when manipulating large displacement, it requires an unnecessary amount

of power to drive the rod. The pin-in-slot mechanism also has difficulty pushing/pulling the rod towards the end of rotation. This mechanism could be replaced with a linear actuator or a servo rack system, which could drive the rod more smoothly and accurately. The current prototype uses an open loop control for actuation. In the future, it could use a closed loop control for enhanced accuracy with integrating flex sensors to the backbone.

**Bibliography**


1. Burgner-Kahrs, Jessica. “Task-Specific Design of Tubular Continuum Robots for Surgical Applications.” *Soft Robotics*, 2015, pp. 222–230., doi:10.1007/978-3-662-44506-8_19.
2. Dong, X., et al. “Development of a Slender Continuum Robotic System for on-Wing Inspection/Repair of Gas Turbine Engines.” *Robotics and Computer-Integrated Manufacturing*, vol. 44, 2017, pp. 218–229., doi:10.1016/j.rcim.2016.09.004.
3. Anderson, V. C., & Horn, R. C. (1967, January). Tensor arm manipulator design. in mechanical engineering (vol. 89, no. 8, p. 54). 345 e 47th ST, New York, NY 10017: ASME-AMER SOC Mechanical ENG.
4. Laschi C, Mazzolai B, Cianchetti M. Soft robotics: technologies and systems pushing the boundaries of robot abilities. Sci Robot 2016;1:eaah3690.
5. RobinsonG,DaviesJ.Continuumrobots—a state of the art Proceedings of the 1999 IEEE International Conference on Robotics and Automation(Cat.No.99CH36288C),Detroit, MI,1999.
6. Albu-SchafferA,EibergerO,GrebensteinM,HaddadinS, Ott C,WimbockT, et al. Soft robotics.IEEERobotAutom Mag 2008;3:20–30.
7. S. Kim, M. Spenko, S. Trujillo, B. Heyneman, D. Santos, M. Cutkosky, Smooth vertical surface climbing with directional adhesion. IEEE Trans. Robot. 24, 65–74 (2008).
8. R. F. Shepherd, F. Ilievski, W. Choi, S. A. Morin, A. A. Stokes, A. D. Mazzeo, X. Chen, M. Wang, G. M. Whitesides, Multigait soft robot. Proc. Natl. Acad. Sci. U.S.A. 108, 20400–20403 (2011)
9. Antonio Bicchi and Giovanni Toniettif. Fast and “Soft-Arm” Tactics. In *IEEE Transactions on Robotics,* June 2004
10. Yu She, Hai-Jun Su, et al. Design and Prototype of a Tunable Stiffness Arm for Safe Human-Robot. In *ASME 2016 International Design Engineering Technical Conference,* August 2016
11. Dong, X., Raffles, M., Guzman, S. C., Axinte, D., & Kell, J. (2014). Design and analysis of a family of snake arm robots connected by compliant joints. Mechanism and Machine Theory, 77, 73-91.
12. K. Suzumori, S. Wakimoto, K. Miyoshi, and K. Iwata, “Long bending rubber mechanism combined contracting and extending fluidic actuators,” IEEE Int. Conf. Intell. Robot. Syst., pp. 4454–4459, Nov. 2013.
13. M. Manti, V. Cacucciolo and M. Cianchetti, "Stiffening in Soft Robotics: A Review of the State of the Art," in *IEEE Robotics & Automation Magazine*, vol. 23, no. 3, pp. 93-106, Sept. 2016.
14. A. Jiang, T. Ranzani, G. Gerboni, L. Lekstutyte, K. Althoefer, P. Dasgupta, and T. Nanayakkara, “Robotic granular jamming: Does the membrane matter?” Soft Robotics, vol. 1, no. 3, pp. 192–201, 2014.
15. Hurd, Carter. “Variable Stiffness Robotic Arm for Safe Human-Robot Interaction Using Layer Jamming.” Thesis. The Ohio State University, 2017. Print
16. Kim J. K, A Novel Layer Jamming Mechanism With Tunable Stiffness Capability for Minimally Invasive Surgery. IEEE Transactions on Robotics, Robotics, IEEE Transactions on, IEEE Trans Robot. 2013;(4):1031. doi:10.1109/TRO.2013.2256313.
17. Du, Z., Yang, W., and Dong, W. (November 1, 2015). "Kinematics Modeling of a Notched Continuum Manipulator." ASME. J. Mechanisms Robotics. November 2015; 7(4): 041017.

18. Dong, X., Raffles, M., Cobos-Guzman, S., Axinte, D., and Kell, J. (November 24, 2015). "A Novel Continuum Robot Using Twin-Pivot Compliant Joints: Design, Modeling, and Validation." ASME. *J. Mechanisms Robotics*. April 2016; 8(2): 021010
19. Al Abeach, Loai & Nefti-meziani, Samia & Davis, Steve. (2017). Design of a Variable Stiffness Soft Dexterous Gripper. Soft Robotics. 4. 10.1089/soro.2016.0044.
20. Mikol, Mikol. "Design, Modeling, and Experimental Testing of a Variable Stiffness Structure for Shape Morphing." OhioLINK ETD: Mikol, Collin Everett
21. Singh, I. (2018, May 1). The design of a cable driven variable stiffness three fingered robotic hand via layer jamming. Retrieved from https://kb.osu.edu/handle/1811/84560.
22. OC Robotics. (n.d.). Retrieved from http://www.ocrobotics.com/technology-/snakearm-robots/.
23. Niu, Guochen, et al. "Attitude Control Based on Fuzzy Logic for Continuum Aircraft Fuel Tank Inspection Robot." *Journal of Intelligent & Fuzzy Systems*, vol. 29, no. 6, 2015, pp. 2495–2503., doi:10.3233/ifs-151952.